Sulfur and carbon controls on methyl mercury in St. Louis River Estuary sediment

Phase II

Dr. Nathan W. Johnson*† and Brian F. Beck†

University of Minnesota Duluth
*Department of Civil Engineering and
†Water Resources Science Graduate Program

8/15/2012

Research Report

Table of Contents

List of Figures

List of Tables

Abstract

The presence of methyl mercury (MeHg) in freshwater aquatic systems is a concern to public health due to its bioaccumulative properties in aquatic food webs and neurotoxicity in humans. Transformation of inorganic mercury to MeHg is primarily driven by sulfate and iron reducing bacteria (SRB and FeRB) in anoxic sediment and water columns. The first objective of this research is to examine the production of MeHg in a sulfate-impacted freshwater estuary in the context of mercury-related geochemical parameters including organic carbon content and lability, sulfate concentrations, and bioavailability of inorganic mercury to methylating microbes. The second objective is to determine the significance of MeHg transport from sediment to the St. Louis River Estuary relative to upstream sources.

A laboratory sulfate addition experiment was performed using 20 cm intact sediment cores obtained from three characteristic sites in the St. Louis River Estuary. The intact cores from each site were exposed to a high (50 mg/L), medium (15 mg/L), and low (5 mg/L) overlying water sulfate treatment for an incubation period of six months. Over the six month laboratory study, MeHg/THg ratios in surface sediment (0-4cm) appeared to be insensitive to overlying water sulfate concentrations in all sites. However, at one site, MeHg/THg ratios in deeper sediment (4-10 cm) did appear to be related to overlying water sulfate concentration. Methyl mercury was strongly correlated with total mercury in sediment from all sites and all sulfate amendment conditions. Analysis of the bulk geochemical differences among sites suggests that MeHg concentrations are related to the total mercury in sediment and the quantity and type of organic carbon.

Laboratory flux measurements provided a means to compare MeHg loading from sediment relative to MeHg loading from the upstream St. Louis River. The estimated MeHg loading from habitat zones represented by the three sites included in this study (45% of total estuary area) exceeds that of upstream sources during median and low flow conditions. These MeHg loading estimates suggest that MeHg transport from sediment could influence overlying water MeHg concentrations in the St. Louis River Estuary.

1. Introduction

Sulfate is elevated in many areas of the St. Louis River Watershed due to historic and ongoing mining operations. (Berndt and Bavin, 2009). Sulfate is of concern in the St. Louis River Watershed not because of its direct toxicological effects but due to its influence on the bioaccumulative form of mercury, methyl mercury (MeHg). Although dominant sources of inorganic mercury vary depending on the aquatic system of interest, it has been widely accepted that atmospheric deposition is a large source of mercury to most aquatic systems (Fitzgerald et al. 1998). In addition to atmospheric sources, the St. Louis River Estuary has been heavily impacted by industrial processes, resulting in localized, high mercury levels (Crane, 2006). The mercury form of greatest interest is MeHg, due to its ability to bioaccumulate in fish tissue and cause neurological damage to humans (Ratcliffe et al. 1996). In the St. Louis River Estuary, there is currently consumption advisory due to elevated fish tissue mercury concentrations (WI DNR. 2011)

The transformation of inorganic mercury to methyl mercury is biologically mediated by sulfate reducing bacteria (SRB) (Compaeu and Bartha, 1985), and requires organic matter, sulfate, inorganic mercury, and anoxic conditions. In fluvial systems, sulfate reduction occurs almost exclusively in sediment, since the overlying water does not favor anoxia (Hammerschmidt et al. 2004[b]; Mitchell et al., 2008a). In low-sulfate freshwater aquatic systems, it has been demonstrated that increasing sulfate concentrations increases the production of MeHg (Gilmour et al. 1992; Jeremiason et al. 2006); however, the biogeochemical processes controlling MeHg production by SRB are complex (Benoit et al. 2003) and involve many factors in addition to sulfate.

The specific area investigated in this study is the lower St. Louis River, a freshwater estuary located at the western tip of Lake Superior which has sulfate concentrations higher than unimpacted waters in the immediate region. In the Estuary, the river width increases considerably, water flow slows, and some exchange of water with Lake Superior occurs in the lower reaches. Since sulfate water concentrations (Berndt and Bavin, 2009) and methyl mercury in fish tissue (WIDnr, 2011) are elevated in the St. Louis River estuary, this study seeks to understand (a) whether elevated sulfate levels are driving methyl mercury production and transport in sediments, and (b) whether transport from sediments represents a significant source of MeHg to the estuary water column. To help answer these questions, laboratory experiments with controlled concentrations of sulfate in the overlying water were conducted on sediments collected from several major habitat zones in the St. Louis River Estuary (St. Louis River Alliance, 2002). Unlike other sediment sulfate addition studies using sediment slurries (Harmon et al., 2007; Gilmour et al., 1992), or episodic additions to field sites (Jeremiason et al. 2006, Coleman Wasik et al. 2012), this study utilized intact sediment microcosms exposed to a constant sulfate boundary condition in the overlying water. The use of intact sediment cores maintains realistic in-situ diagenetic redox zones and relies on diffusional transport to move sulfate into sediments, thus providing conditions analogous to those encountered in a freshwater estuary sediment environment.

2. Background

Sediment Diagenesis

In aquatic sediments, the consumption of oxidized compounds acting as electron acceptors occurs in a sequential pattern at increasing depth in the sediment (Froelich et al., 1979). Due to differences in Gibbs free energy associated with each reaction, the characteristic order of electron acceptor consumption in sediment is oxygen (O_2), nitrate (NO_3^-), manganese (Mn^{4+}), ferric iron (Fe^{3+}), and sulfate (SO_4^{2-}) (Stumm and Morgan, 1996). The reduction of electron acceptors in sediment is primarily driven by heterotrophic bacteria which utilize organic carbon as an electron donor during metabolism (Jorgensen, 1982).

The primary driver of sediment diagenesis in freshwater and marine sediments is organic carbon flux into sediment (Meyers and Ishiwatari, 1993). In sediment systems that are organic rich, accelerated rates of microbial activity tend to compress microbial communities upwards, near the sediment water interface. Conversely, in organic poor aquatic systems, redox zones are stretched out, allowing the penetration of oxidized electron acceptors deeper into sediments (Katsev et al. 2006). In addition to concentration of organic carbon, the recalcitrance of the available organic carbon pool can limit or accelerate microbial processes (Meyers and Ishiwatari, 1993). The type of organic carbon transported to the sediment can be placed in two general categories, autocthonous and allocthounous carbon (Wetzel, 2002). Autochthonous carbon, which is typically considered the more labile of the two types of carbon, is produced at or near the site of consumption. Organic carbon produced outside the system of interest is considered allocthonous organic carbon (Wetzel, 2002). Since organic carbon in fluvial systems can be degraded during transport by microbial and macrobiotic processes, allocthonous carbon (produced elsewhere) tends to be more refractory (Vannote et al. 1980). Both the magnitude and type of organic carbon play major roles in controlling the rates of sediment diagenesis.

In addition to microbially driven reactions in the sediment column, abiotic reactions influence porewater and solid phase geochemistry. Abiotic processes that have an important role in sediment geochemistry are secondary redox, complexation, and precipitation/dissolution reactions. Secondary redox reactions involve many byproducts of microbial reduction reactions and oxidized species (Fossing et al., 2004). Certain electron acceptors are immobile while in their oxidized form (ferric iron and manganese(IV)), but are mobilized (ferrous iron, manganese (II)) once reduced by microbial communities (Brown et al. 2000). These reduced chemicals can diffuse into more oxidized zones and react with electron acceptors (Fossing et al., 2004). In addition to secondary redox reactions, complexation reactions have the ability to limit or enhance the reactivity or mobility of dissolved species and some complexation reactions produce a solid phase precipitate (sulfide-iron(II) precipitation to solid phase FeS). This collective sequence of reactions, including biologically mediated electron acceptor reduction and reactions among byproducts of microbial metabolism, is termed diagenesis.

Methyl mercury Production and Demethylation

The transformation of inorganic mercury to methyl mercury has been shown to be a biologically mediated process (Compaeu and Bartha, 1985; Gilmour et al., 1992; Kerin et al., 2006; Fleming et al.,

2006). Sulfate reducing bacteria are widely considered the primary methylators of mercury in aquatic sediment (Gilmour et al. 1992; Jeremiason et al. 2006), while iron reducing bacteria have demonstrated the ability to methylate mercury in pure cultures (Fleming et al., 2006; Kerin et al., 2006). For sulfate reduction to occur, anoxic sediment conditions must be present. Otherwise aerobic bacteria out compete SRB.

In environmental systems, MeHg is also demethylated through biotic and abiotic processes. The balance between coincident methylation and demethylation processes results in a steady state MeHg concentration in sediment (Drott et al. 2008). Microbial MeHg degredation is thought to be the most important demethylation process in sediment (Benoit et al. 2003), and abiotic demethylation pathways, including photodegredation and oxidative demethylation, contribute to a lesser extent in sediment (Sellers et al. 1996; DiPasquale et al. 2000). It has been observed that %MeHg in the solid phase is a good measure of net MeHg production in sediment systems while instantaneous measurements of MeHg production rates, (k_m) measured through spikes of enriched stable isotopes, is much better short term indicator (Drott et al. 2008).

Sulfate limitation

A number of studies have investigated sulfate limitations in fluvial sediment and wetland systems by testing whether sulfate addition alone can stimulate mercury methylation (Braunfireun et al. 1999; Gilmour et al. 1992; Jeremiason et al. 2006; Harmon, 2004). Since SRB are the primary methylators of mercury in many environmental systems, sulfate addition to an anoxic systems starved for sulfate often increases SRB activity, thereby enhancing methyl mercury production (Benoit et al., 2003). A number of proxies and measures for increased SRB activity can be used to assess the magnitude of SRB response to sulfate additions including sulfate reduction rate (SRR), microbial community characterization, sulfide concentrations, CO_2/CH_4 production, and AVS (King et al. 1999; King et al. 2000; Benoit et al. 2003).

A number of sediment sulfate addition experiments have been conducted in homogenized sediment amended with sulfate (sediment slurries) or pure cultures of particular SRB (Harmon et al. 2004; Gilmour et al. 1992; King et al. 2000). These studies have been useful in determining some of the biological mechanisms behind MeHg production in sediment but do not replicate intact diagenetic redox zones encountered in many field conditions. There have also been studies examining field scale sulfate additions to a wetland system which demonstrated significant MeHg response to episodic sulfate additions (Jeremiason et al. 2006, Coleman-Wasik et al. 2012). While performed under field conditions, the sulfate loading in these studies is not representative of constant increased loading of sulfate to sediment from the water column.

Although production of MeHg is limited by sulfate in many freshwater systems, a complex set of factors influences the production of MeHg (Harmon et al. 2007). Factors such as labile organic carbon availability, porewater inorganic mercury bioavailability, and competition among microbial communities can alter biogeochemical dynamics, creating situations in which an alternate set of limiting factors may arise (Hammerschmidt and Fitzgerald 2004a; Drott et al. 2007; Todorova et al. 2009;). A conceptual model more complex than simple sulfate driven MeHg production is required to adequately explain

mercury dynamics in sediment.

Mercury Porewater Bioavailability

Of all mercury present in aquatic sediments, typically less than 0.1% is present in sediment pore fluids, while the remainder is bound to the solid phase (Fitzgerald et al. 2007). The small amount of mercury present in the pore fluid is important, however, since it is the mobile fraction and able to participate in chemical and biological reactions. Porewater speciation of inorganic mercury is thought to have a large influence on the ability of a given system to produce MeHg efficiently (Benoit et al. 2003). Observations of systems with elevated dissolved sulfide concentrations and muted MeHg production provided early evidence of sulfide's influence on MeHg production (Gilmour et al. 1998; Benoit et al. 2001). Geochemical equilibrium modeling suggests that high sulfide concentrations can lower the concentration of uncharged mercury-sulfide complexes (primarily HgS^0), which may diffuse passively across the membranes of SRB (Benoit et al. 1999[a]). The mercury-sulfide neutral-complex model is well supported (Gilmour et al. 1998; Benoit et al. 1999[a]; Benoit et al. 1999[b]; Benoit et al. 2001; Benoit et al. 2003), but the values of equilibrium constants used for the model are not well known (Skyllberg, 2008; Drott et al. 2007), especially in relation to equilibrium constants for organic matter thiol groups, another important ligand for inorganic mercury (Skyllberg et al. 2006). Low molecular weight organic compounds are capable of complexing mercury and may be transported into methylating bacteria via active transport (Golding et al. 2002). SRB culture studies (Graham et al. 2012; Schaefer et al. 2011; Schaefer and Morel 2009) and DOM modeling (Skyllberg, 2008) have demonstrated that DOM can significantly increase the bioavailability of inorganic mercury and production of MeHg in some systems. Iron sulfide complexes may also have a role in limiting the bioavailability of porewater inorganic mercury (Skyllberg, 2008, Skyllberg and Drott 2010). Experimental additions of pyrite have demonstrated iron sulfide solids have the ability to remove inorganic mercury from solution (Bower et al. 2008) and inhibit MeHg production (Liu et al. 2009).

Organic Carbon Limitation

Organic carbon is the basic metabolite for all chemoheterotrophic bacteria and is used as an electron donor (Froelich et al. 1979). Low quantities of labile organic carbon can limit the production of MeHg in sediments if a sulfate limitation has not been imposed on a system (Mitchell et al. 2008[a]). The addition of labile organic carbon to a system that is known not to have a sulfate limitation can yield high mercury methylation (Mitchell et al. 2008[a]). Carbon to nitrogen ratios can be used to determine the overall origins (autochthonous or aullocthonous) of the organic carbon in a system and infer the capacity to drive microbial metabolism (Kim et al. 2011). .

Solid phase organic carbon also binds mercury strongly and can inhibit the production of MeHg in sediments by lowering inorganic mercury in pore waters. In many systems, organic carbon is inversely correlated with porewater mercury, the fraction of the inorganic pool which is mobile and potentially available to methylating microbial populations (Hammerschmidt and Fitzgerald 2004a). Understanding the recalcitrance of the total carbon pool can assist with interpreting carbon's role in driving microbial activity and carbon's role in binding inorganic mercury (Kim et al. 2011).

Transport from sediments

Many studies have sought to quantify the transport of inorganic and methyl mercury from sediments to the overlying water. Some have made direct measurements (in situ: Gill et al. 1999[a], Benoit et al. 2009; or lab incubations: Covelli et al. 2008, Hammerschmidt et al. 2008a) and some have used estimates of sediment diffusion based on observed porewater concentrations (Hammerschmidt et al. 2008b). In general, estimates of flux from diffusion calculations have been lower than total flux measured in-situ or in lab measurements; however in some cases experimental measurements of total fluxes are smaller than diffusion estimates from porewater concentrations (Gill et al. 1999[a], Choe et al. 2005). Total MeHg fluxes vary widely (from -100ng/m2/day to +2000ng/m2/day) and have been shown to vary seasonally (Corvalli et al. 1999) and even diurnally (Gil et al. 1999a) owing to factors including bioturbation (Benoit et al. 2009), redox boundary layers (Covelli et al. 1999), and dominant speciation (Jonsson et al. 2010). Recently, it has been suggested that sulfide may outcompete organic ligands for methyl mercury at high sulfide concentration and low pH (Jonsson et al. 2010). Although the complexation constants that predicts the predominance of methyl mercury bisulfide (CH_3HgHS^0) at high sulfide concentrations were not measured directly (Dyressen and Wedborg 1991), the species would exist as an uncharged molecule and have a substantially higher potential for transport with faster aqueous diffusion and potential for partitioning into dissolved gasses (Berndt and Bavin, 2011; Gray and Hines, 2009).

3. Experimental Design and Methods

Site Selection

The St. Louis River Alliance has outlined habitat zones which delineate and categorize zones of similar aquatic habitat type (St. Louis River Alliance, 2002). Representative sites for collecting sediment for the laboratory study were selected by choosing locations that (a) are within habitat zones that cover a large portion of the estuary, (b) are not influenced by regular dredging operations in the working harbor, and (c) have a range of organic carbon quantity and quality. Sites were chosen from the Lower Estuary Flats (LEF, 21% of estuary area), Upper Estuary Flats (UEF, 16% of estuary area), and Sheltered Bays (SB, 8% of estuary area). The three sites selected were in habitat zones that covered a total of 45% of the St. Louis River Estuary. Other habitat zones did cover a larger portion of the estuary but they were either highly influenced by industry or were located in the portion of the estuary that is regularly dredged, both factor that present a challenge to representative sampling. The LEF and SB habitat zones had prior information about bulk geochemical conditions, which demonstrated that there was a range of solid phase organic carbon (<2% to ~6% TOC, respectively, Johnson and Beck (2011)).

Study Design and Field Methods

Sediment cores were collected from a small boat during August, 2011 using a custom designed sediment corer consisting of a 20 cm inner diameter polycarbonate tube. The sediment corer (Figure 3) was driven into the sediment using a drive rod operated by staff on the sampling boat. Once the core tube had penetrated 20-30 cm into the sediment, two ball valves were shut (ball valves remained open while core tube is driven into sediment) to create a hermetic seal that would preserve the sediment

water interface within the core tube once the core was removed from sediment. As the core was removed from the sediment, the bottom was capped immediately by a diver with an o-ring fitted polyethylene disk.

All twelve sediment cores were transported back to the laboratory where dissolved oxygen and pH were measured in the water overlying the sediment. Subsequently, two holes were drilled into the polycarbonate tubing 10 cm above the sediment water interface directly across from one another and fitted with 1/4" hose barbs. Within 4 hours of collecting cores, oxygenated water from each respective sample site was flowing over the sediment cores at 100 mL min^{-1} to ensure the water near the sediment water interface would not become anoxic. Microcosms were then allowed to equilibrate at the incubation temperature (20 ^{o}C) for one week before any lab analysis was performed.

After a one week period, initial conditions for the sulfate addition experiment were measured in each microcosm using replicate voltammetric electrodes for redox-active species (Mn^{2+}, Fe^{2+}, total dissolved S^{2-}, and O_2) sediment porewaters and triplicate sub-cores to obtain samples solid phase and other porewater chemicals. The same methods were used to analyze the final conditions of the microcosms after the 6 month microcosm incubation. In an effort to reduce variability among cores, biota (zebra mussels and worms) were actively removed from the laboratory microcosms.

Once initial conditions for each microcosm were characterized, carboys containing water from each field site were disconnected from the peristaltic pump and connected to a reservoir of natural water amended with sodium sulfate. Each habitat zone had three different overlying water sulfate treatments applied for a period of 6 months. All treatments used water from the Cloquet River, since it has similar dissolved organic carbon concentrations to the main stem of the St. Louis River (10-20mg/L DOC) and low sulfate concentrations (2.5-5 mg L^{-1}) (Berndt and Bavin, 2009). The three overlying water treatments applied to each habitat zone contained high (50 mg L^{-1}), medium (15 mg L^{-1}), and low (5 mg L^{-1}) sulfate concentrations which simulated environmentally relevant sulfate concentrations in the St. Louis River Estuary (Figure 2). The medium (control) concentration was picked by estimating the sulfate concentration at the median discharge near the beginning of the St. Louis River Estuary in Cloquet, MN where a USGS continuous stream gauging station is located (Scanlon, #0402400). The median discharge at the gauging station for August (1,290 ft^3 s^{-1}) was then compared to discharges and sulfate concentrations measured by Berndt and Bavin (2009) to determine an average sulfate concentration that would be used for the medium (control) treatment (15 mg L^{-1}). The low treatment (5 mg L^{-1} sulfate) was chosen based on observations in local, unimpacted tributaries, such as the Cloquet River (Berndt and Bavin 2009). Chloride was also added to the overlying water as a tracer (at concentrations 10-20x higher than in-situ observations) to ensure that diffusional transport was effectively delivering chemicals from the overlying water to sediment over the timescale of the experiment.

The reservoir of high sulfate water was used to recirculate water over the LEF high sulfate treatment, the UEF high sulfate treatment, and the SB high sulfate treatment. Similarly, medium and low sulfate reservoirs were recirculated over the respective microcosms from each habitat zone. Weekly monitoring of sulfate concentration in reservoirs ensured sulfate remained at initial concentrations. Fresh Cloquet water was obtained every two months during the experiment.

Laboratory Experimental Methods

In order to make destructive measures of solid phase and porewater chemicals, sub-cores were collected from experimental microcosms in triplicate using one inch inner diameter polycarbonate tube. Before the 1 inch polycarbonate tubing was inserted, a 1 3/16 inch butyl tube was inserted into the sediment to prevent surrounding sediment from falling into the void created after removing a sub-core. Following extraction, sub-cores were immediately extruded using a 7/8 inch polyethylene rod wrapped with electrical tape to ensure a secure fit inside the sub-coring tube. Sediment was sectioned into 0-4 cm, 4-10 cm, and 10-20 cm intervals and placed directly into VWR trace metal clean glass jars. Each sediment sample jar was immediately filled with nitrogen to ensure that sediment redox conditions were not altered significantly. Within 15 minutes of sub coring sediment, samples were placed in a Coy glove box with an oxygen free atmosphere (97.5% nitrogen and 2.5 % hydrogen) where samples were homogenized and subsampled for solid phase and porewater analysis. All solid-phase samples that were not analyzed within 12 h of sub-coring were placed in a -20^{o} C freezer until analysis.

To preserve the integrity of the experimental microcosm during initial sub-coring, the voids left from the extracted sub-cores were filled with sediment from a sacrificial sub-core taken from a fourth, sacrificial microcosm from each site. To ensure that sediment added to the experimental microcosms from the sacrificial microcosm was not substantially different relative to the experimental objectives, the sacrificial microcosm was also analyzed to determine its solid phase and porewater chemistry. To determine the variability within each habitat zone, triplicate one inch sub-cores were analyzed separately for one microcosm from each habitat zone. In the other two microcosms that did not have triplicate sub-cores analyzed separately, triplicate sub-cores were composited at each respective depth (0-4, 4-10, and 10- 20 cm).

Sediment THg and MeHg partitioning coefficients (K_D [L/kg]) are defined as the ratio of total solid phase mercury [ng/kg] to porewater mercury [ng/L] (passing 0.45um filter) and were determined for each habitat zone at the close of the experiments. A 2.5" polycarbonate sub-core was removed from each microcosm and the top 10cm extruded into a 1 gallon Ziploc sample bag, transferred into an anaerobic glove box, and homogonized. Each homogenized sediment sample was transferred into 50 mL polypropylene centrifuge tubes (multiple required per microcosm), centrifuged at 10,000 rcf for 30 min, and filtered through a 0.45µm polyethersulfone filter (VWR, Supor). Water samples were filtered into clean PETG bottles and acidified (0.5%) using ACS trace metal grade hydrochloric acid. A small aliquot of homogenized sediment was also removed prior to centrifugation and placed in a VWR trace metal clean scintillation vial for solid phase analysis.

Flux experiments were conducted at the end of incubations to determine the magnitude of mercury flux out of sediment from each habitat zone. To conduct these experiments, fresh water from the Cloquet River was obtained in 50 L carboys. To remove any previous overlying water, five volumes of new water were allowed to flow over each microcosm to ensure fresh Cloquet River water was present on top of each microcosm. After fresh water was supplied to the overlying water of each microcosm, pumping was stopped, and water remained on top of sediment for 36-48 hours under well-mixed conditions created by a slow bubble of air. Overlying water was collected at the beginning and end of flux experiments using acid cleaned polypropylene syringes and immediately filtered using

disposable 0.45 µm polyethersulfone filters directly into PETG trace metal clean bottles. Flux experiment water samples were acidified with 0.5% trace metal hydrochloric acid.

Analytical Methods

Porewater

Porewater sulfide, the sum of H_2S and HS^- (denoted ΣS^{2-}), ferrous iron (Fe^{3+}), and manganese (Mn^{2+}) were measured with mercury gold amalgam voltammetric electrodes using methods similar to Brendel and Luther (1995). A Cloquet River water matrix was used to calibrate electrodes for Mn^{2+} and Fe^{2+} at pH 4.5 with 0.6 mM and 1.2 mM acetic acid buffer, respectively. Sulfide calibrations were conducted in a 1.2 mM HEPES buffer (pH 8.6) in a Cloquet River water matrix. A two point oxygen calibration was performed in Cloquet River water assuming zero oxygen after nitrogen purging and equilibrium oxygen concentrations with atmospheric conditions after air bubbling. All anoxic calibration (Mn^{2+}, O2, Fe^{2+}, and S^{2-}) solutions were degassed by purging the solution with nitrogen gas at 80 cm^3min^{-1} for 20 minutes and maintaining nitrogen headspace during analysis. Square wave voltammetric scans were used for ΣS^{2-}, Mn^{2+}, and Fe^{2+}, and consisted of a potential range of -0.1 to -2.1 volts (V) vs silver/silver chloride (Ag/AgCl) reference electrode, 15 mV step height, 200 mV s-1, and 2.25 mV step increment. In the presence of ΣS^{2-} a -0.8 V conditioning step was applied before the acquisition scan, while in the presence of Mn2+ and Fe2+ a -0.2 V conditioning step was applied for 10-30 seconds to remove any iron, manganese, or sulfur deposited during scans. Oxygen was determined with linear sweep voltammetric scans with a range of -0.1 to -1.8 mV and 200 mV s-1 scan rate.

Porewater samples for other analytes (sulfate and DOC) were obtained by placing an aliquot of sediment from a sub-core section into a 50 mL centrifuge tube under an N_2 atmosphere and centrifuging at 10,000 rpm for 30 minutes. Samples were then filtered through 0.45 µm polyethersulfone filters directly into acid cleaned 15 mL polypropylene centrifuge tubes and stored short-term in an N_2 atmosphere to avoid oxidation. A 5-10 mL aliquot of filtered porewater was acidified to pH 4.5 using 0.1 N nitric acid to convert all dissolved sulfide species (H_2S , HS^-, and S^{2-}) to H_2S, and prevent sulfide oxidation to sulfate. Acidified samples were purged of dissolved gas by bubbling with oxygen free nitrogen gas. Sulfate and chloride samples were analyzed by ion chromatography on a Dionex ICS-1100 IC system (IonPac AS22 4x250mm column) connected to an AS-DV Autosampler. Samples for dissolved organic carbon (DOC) were acidified to pH 2 to remove any dissolved inorganic carbon (DIC) and analyzed in a Shimadzu TOC_{VSH} high temperature carbon analyzer with a sparging time of 3.5 min.

Solid Phase Analysis

All solid phase sediment that was analyzed on a wet basis (AVS and Ferrous Iron) was normalized by a dry/wet weight ratio. A quantitative mass of sediment was weighed in an aluminum weight dish and heated to 105 ^oC for 24 hours to dry completely. Once dried, it was weighed again to obtain the dry weight and percent solid content of each sample. Each sediment section was analyzed separately for percent solid content to ensure that all solid phase samples were normalized correctly.

Acid Volatile Solids (AVS) was measured in the sediment solid phase using the Brower diffusion method (Brower and Murphy, 1994) and quantified with an Ion Selective Electrode (Eaton et al. 2005).

Solid Phase ferrous iron was extracted using an oxalate extraction outlined in Phillips and Lovley (1987). Total sulfur (TS) and total carbon (TC) sediment samples were dried for 48 hours in a 60^{o}C oven to remove any moisture and quantified with thermal conductivity in a CHN analyzer. SRB abundance was characterized by quantitative real time polymerase chain reaction (qPCR) using a Mo Bio Powersoil extraction kit. Methods for analysis and quantification of the sediment extraction results are outlined in Schippers et al. (2006) as modified by Hicks and Oster (2012).

Methyl mercury and total mercury sediment aliquots were removed from the original sample container before all other analytes and placed in VWR trace metal cleaned glass scintillation vials in an oxygen free atmosphere. An acid-cleaned Teflon spatula was used to transfer sediment for mercury analysis. Samples were placed in a freezer (-20^{o} C) within 30 minutes of sub-sampling sediment core sections. Before analysis, sediment was freeze dried at the lab in which it was analyzed. Total- and methyl- mercury analysis was performed by the University of Toronto using isotope dilution ICP-MS and analytical methods are outlined in detail in Mitchell and Gilmour (2008[b]), Hintelmann and Evans (1997), Hintelmann and Ogrinc (2003), and Horvat et al. (1993).

4. Results and Discussion

Geochemical setting

Differences in sediment carbon content and quality are illustrated in Figures 4a and 4b for each of the LEF, UEF, and SB habitat zones. Abundant carbon is capable of driving fast rates of diagenetic activity if the carbon is present in a labile form (Kim et al. 2011). The SB had more abundant solid phase TC concentrations (4-6% TC) relative to LEF and UEF (2-4% TC) (Figure 4a). In the SB and UEF sites, TC decreases with depth suggesting a continuous supply of depositional carbon that is consumed during burial. Dissolved organic carbon concentrations in sediment pore water did not differ among habitat zones and were relatively consistent with depth in the SB (24.5±0.5 mg/L DOC), LEF (22.8±4.5 mg/L DOC), and UEF (26.2±5.9 mg/L DOC) sediment.

C/N ratio can be used as a proxy for the recalcitrance and source of organic carbon in sediment. In the water column, freshly produced particulate organic carbon (POC) exhibits C/N values of 6-11 (Kim et al. 2011). In the SB habitat zone, C/N ratios (12.8-15.0) were slightly higher than values characteristic of freshly produced organic matter. The observation that C/N ratios (indicating carbon recalcitrance) increase with depth in SB and UEF sediment suggests that labile carbon is degraded in surficial sediment during burial. C/N ratios demonstrate that organic carbon in the LEF sediment is more recalcitrant than that in the SB and UEF sediment which may lead to lower microbial activity. Since the carbon that is delivered to the LEF sediment appears to be recalcitrant, the consequent slower microbial utilization of this carbon would explain the lack of a significant increase in C/N ratio with depth.

Despite areas of localized mercury contamination in the estuary, total mercury in the sites sampled is not highly contaminated (>500 ng/g THg) (Benoit et al. 2003) but is higher than many sites impacted only by atmospheric deposition (Fitzgerald et al. 1998). The study sites have significant differences in total mercury (THg) concentrations with the more organic rich SB sediment containing the

highest concentrations (260±102 ng/g). The LEF and UEF have lower THg concentrations of 112.3±49.9 ng/g and 70.7±26.5 ng/g, respectively. Solid phase total mercury was the most variable in cores collected from the LEF habitat zone and exhibited a significant decreasing trend with depth and variability amongst cores. Sediment solid phase THg concentrations agree with the first year bulk geochemical analysis of THg in the LEF and SB sites (Johnson and Beck, 2011).

Experimental Results and Discussion

Sulfate and Chloride

At the beginning of incubations, sulfate penetrated to a sediment depth of 5-10 cm in all treatments, indicating that sulfate reduction is occurring in this zone in all habitat zones (Figure 5 a-c). After the 6 month incubation, sulfate penetration into the sediment was greater in the high sulfate treatments (20-30 mg/L at 2cm depth; 1-4 mg/L at 7 cm depth) relative to the medium treatment (5-10 mg/L at 2 cm depth; <0.1 mg/L at 7 cm depth) and low treatment (0.1-3.8 mg/L at 2 cm depth and <0.1 mg/L at 7 cm depth). To ensure that there was a diffusive flux into the sediment, chloride was added to the overlying water as a conservative tracer at a concentration of 200mg/L. The initial (uniformly (9.6 ± 1.1 mg/L)) and final (150-200mg/L) porewater chloride profiles indicate that diffusion effectively transported chloride from the overlying water to 20cm depth in experimental microcosms over the 6 month experiment. Chloride and sulfate observations (Figure 5) demonstrate that sulfate reducing bacteria in surface sediment were exposed to varying amount of sulfate which was a main objective of the experiment design. However, the resolution of sulfate measurements makes it difficult to ascertain the depth at which sulfate reduction began in sediment.

Porewater Redox Conditions

Initial and final porewater profiles for redox-active dissolved chemicals are shown in Figures 6 and 7. For Figures 6-7, the rows of figure panels correspond to different habitat zones (a-c LEF; d-f UEF; g-i SB). Columns of figure panels correspond to different sulfate amendments (a,d,g low; b, e, h medium; c, f, i high). Initial porewater measurements of ΣS^{2-}, Fe^{2+}, and Mn^{2+}, illustrate a clear geochemical difference between the sediment from flats habtat zones (LEF / UEF), and the SB habitat zone. Porewater in LEF and UEF habitat zones have high Mn^{2+} (200-350 uM) with no detectible Fe^{2+} or ΣS^{2-} (Figure 6a-f) and are similar for all sediment microcosms. A sediment profile consisting of Mn^{2+} with no detectable Fe^{+2} or S^{2-}, suggest the LEF and UEF habitat zones have less labile or lower concentration of organic carbon (effectively stretching redox boundaries to deeper depths) or a limited supply of Fe^{3+} and sulfate. In SB sediments (Figure 6 g-i), porewater Fe^{2+} concentrations were high in porewaters (200-400 uM) (Figure 6g-i), with small amounts of detectible ΣS^{2-} (1-5 uM). The SB habitat zones are backwater sites, which leads to hydrologic conditions similar to lakes and the potential for anoxia in the water column. An oxygen-depleted hypolimnon could lead to Mn^{2+} transport to the overlying water (in the absence of oxygen) allowing iron and sulfate reduction to move into the surficial sediment. A higher abundance of labile organic carbon in the SB habitat zone, in conjunction with periodic anoxic overlying water could be responsible for a shift upward in iron and sulfate reduction relative to UEF and LEF sites (Figure 6).

The final porewater concentrations for redox-active chemicals in the LEF and UEF sediment did not change relative to the initial conditions (Figure 7a-f). Porewater concentration for redox active chemicals changed markedly in the SB habitat zones from the initial to final sampling (Figure 7g-i). Porewater Mn^{2+} concentrations in SB sediment were below detection limit in the initial conditions while it increased to 100-200 uM in the final conditions. This change in redox conditions was most likely driven by a change in overlying water oxygen concentrations. The field conditions of the overlying water may have been anoxic due to a thermal stratification and significant sediment oxygen demand. After pumping water saturated with oxygen over the sediment for 6 months and altering the redox boundary at the sediment water interface, the less thermodynamically favorable reduction reactions (iron and sulfate reduction) appear to have been lowered in the sediment column (Figure 7g-i). Changing redox conditions can change the locations and activity of microbial communities that mediate the production of MeHg (Johnson et al. 2010).

Solid Phase Redox Conditions

Figures 8-11 contain initial and final solid-phase sediment concentrations of AVS, %TS, Fe2+, and SRB abundance. In each of these figures, initial conditions are depicted with dotted lines and final concentrations with solid lines. Columns of panels contain concentrations from each habitat zone, while rows represent different sulfate amendment levels in the overlying water. The AVS extraction method quantifies the least recalcitrant pool of solid phase iron sulfide minerals (FeS), while not measuring pyrite (Fe_2S), and can be considered the more recently formed or loosely bound iron sulfide minerals (Brouwer and Murphy 1994). Initial conditions for AVS (Figure 8) show that sediment from the SB habitat zone has the greatest abundance of solid phase AVS (Figure 8 b, e,h) with a peak near the sediment water interface (SWI) (50±2.4 umol/g dw) and a decrease with depth (to 8.0±2.4 umol/g dw). An opposite AVS profile is seen in the sediment from the LEF and UEF habitat zones, where higher concentrations occur deepest in the sediment profile (Figures 8 a, d, g; c, f, i). The increase of AVS with depth in sediment from UEF and LEF habitat zones, suggests slow accumulation of loosely bound, reduced iron sulfides during burial.

For SB microcosms, the concentrations 6 months after amendments display a marked change in AVS in surficial sediment which is consistent with porewater redox changes observed in voltammetric electrode measurements (Figure 7) and decreases in total sulfur in the 0-4 cm interval (Figure 9, 30 umol/g ~0.1% S). The surficial sediment (0-4 cm) appears to have been exposed to less reducing conditions leading to the oxidative dissolution of iron sulfide minerals, while deeper areas in the sediment (>10cm) appeared not to be affected by this change to the upper boundary condition. Sediment between 4-10cm had an increase in AVS relative to initial conditions in high and medium sulfate amended microcosms. The oxidation of iron sulfide minerals may have created a situation in which both internal loading of sulfate from the sediment and external loading of sulfate (diffusion from overlying water) were significant. For LEF microcosms, little change was observed in AVS following the 6 month incubation, but slight decreases were observed at depth for low and medium sulfate treatments below 4cm (Figure 8a, d, and g). AVS in sediment from the UEF habitat zone increased relative to the initial conditions for all sulfate treatments between 4-10cm and for low and medium sulfate treatments

between 10-20cm. Although one explanation for this increase is sulfate diffusion from the overlying water, reduction and immobilization, a parallel increase in TS was not observed in UEF sediment (Figure 9) and would have been quantifiable (20umol/g ~0.06%). Additionally, estimates of sulfate diffusion based on observed gradients are far less than necessary to account for the increase of AVS over 4-10cm. It is possible, therefore that over the course of the experiment, recalcitrant iron sulfide minerals, such as pyrite, were transformed into more labile reduced species that AVS is capable of measuring.

Measurements of total sulfur (TS), which quantifies all sediment sulfur, is presented Figure 9. The SB sediment solid phase TS (Figure 9, panels b, e, h) follows a similar trend as AVS for the initial and final experiment conditions (Figure 8). For sediment underlying a seasonally anoxic water column, this similar behavior between TS and AVS might be expected in surficial sediment as recalcitrant solid phase iron sulfides (resistant to AVS extraction) require permanent anoxic conditions to form. There was a decrease relative to initial conditions in TS from 0-4 cm in the low and medium LEF sulfate treatments but no change in the high LEF treatment. TS was not measured initially in the UEF high sulfate treatment sediment. However, if assumed to be similar to initial TS content in medium and low sulfate treatment sediment, an increase in TS was observed between 0-4 cm and 4-10 cm relative to initial conditions (Figures 8c, f, and i).

Ferrous iron was measured in the solid phase and is depicted in Figure 10. Solid phase Fe^{2+} increased between 4-10 cm in all SB treatments relative to initial conditions (Figure 10b, e, and h) likely due to a redox change in the upper oxygen boundary, not a result of sulfate treatments. As discussed previously, the release of iron sulfide minerals could produce ferrous iron that can be measured with the extraction method used in this study. Porewater Fe^{2+} concentrations decreased from the initial conditions (Figure 6 g-i), implying that there was not an increase in iron reduction in the SB sediment. Little change was seen in solid phase Fe^{2+} for the top 10cm of LEF microcosms over the course of the study, while increases were observed from 10-20 cm (Figure 10). The UEF high treatment sediment in the 0-4cm interval displayed a marked decrease in solid phase ferrous iron, although it began with a magnitude four times larger than any other sediment microcosm (Figure 10).

Sulfate Reducing Bacteria Microbial Abundance

The abundance of sulfate reducing bacteria (SRB) was measured in the solid phase and is displayed in Figure 11. In the high-sulfate treatments for all habitat zones, the top 4 cm displayed an increase in SRB abundance relative to initial conditions and data suggests that this increase was statistically significant for SB and UEF microcosms (Figure 11 b and c). For the medium sulfate treatments, SRB abundance in the 0-4cm interval increased relative to initial conditions for LEF and UEF sediment, but remained similar in SB sediment. For low sulfate treatments, a decrease in SRB abundance relative to initial conditions was observed at all depths for SB sediment, but UEF and LEF showed little difference from initial conditions.

Mercury Experimental results

Solid phase THg concentrations varied among habitat zones and even among cores collected from the same habitat zone, (Figure 12, 13 and 14). Differences were most notable for microcosms collected in the LEF habitat zone, but also were present in the initial UEF medium (higher THg between 0-4 cm). Variability in total mercury necessitates normalization of the MeHg data to total mercury concentration if treatments are to be compared to one another in terms of methyl mercury production efficiency. In sediments that are not highly contaminated with mercury (<500 ng/g), MeHg and THg are often strongly correlated (Figure 15). A strong correlation was observed in this study, suggesting that no sediment conditions (among all habitat zones and overlying water sulfate amendments) were producing methyl mercury much more efficiently than others. A unit commonly employed to determine a sediment's capacity to methylate mercury under its in-situ geochemical setting is %MeHg (Drott et al. 2008). Since %MeHg is a measure of the sediment's capacity to methylate mercury, it will be used exclusively to compare limiting factors in the production of MeHg. Sediment profiles of MeHg, %MeHg, and THg are displayed in Figure 12, 13 and 14 for the initial treatments and treatments after 6 months. Error bars represent one standard deviation from the mean as calculated by the analysis of triplicate sub-cores from each habitat zone at the beginning of experiments. Panels a-c give concentration at the end of the experiment and panels d-f show initial conditions.

In sediment from the LEF habitat zone, %MeHg in the 0-4cm interval appeared to be unrelated to overlying water sulfate after the 6 month lab experiment (Figure 12b); however, %MeHg in the 4-10cm interval was consistent with increased with increasing overlying water sulfate. Although SRB abundance was not related to overlying water sulfate concentrations in LEF sediment (Figure 11), the increased %MeHg in the 4-10cm interval is consistent with SRB-driven methylation below the oxidized surface layer of sediment.

In sediment from the SB habitat zone % MeHg was not significantly different than the initial conditions in the high, medium, or low sulfate treatments ($p > 0.05$) and did not differ amongst sulfate treatments (Figure 13). The SB has the greatest abundance of AVS and SRB suggesting that there is SRB mediated sulfate reduction producing MeHg in the sediment. However, the oxidation of reduced sulfides in the top 10 cm as a result of experimental manipulation likely caused internal loading of sulfate which could have lessened the influence of overlying water sulfate. Although this was an artifact of the experimental design, it may reflect conditions in the field if periodic anoxia exists in the bottom waters of SB environments. There was a clear decrease in sulfate reducing bacteria in the surficial sediment of the SB low sulfate treatment (Figure 11) which suggests that sulfate in the overlying water did influence SRB. However, a coincident decrease in %MeHg was not observed, suggesting that other factors such as the availability of inorganic mercury to methylating microbes may be limiting methyl mercury production in sediment of the SB. The SB sediment did have the lowest

porewater total mercury concentrations of any habitat zone despite the highest solid-phase total mercury (Table 3).

In the initial and final experimental conditions, sediment from the UEF habitat zone had higher %MeHg concentrations (Figure 12, 13, and 14) than sediment from other habitat zones at all depth intervals. The low UEF sulfate treatment displayed a large increase in %MeHg in the 0-4cm interval (Figure 15) relative to initial conditions, though geochemical trend analyses indicate that this point may be an outlier when compared to the entire data set (Figures 17 and 18). There was a clear increase in SRB abundance in the high sulfate treatment at all depths (Figure 11c) which was not coupled to an increase % MeHg (Figure 14b). A sediment system in which methyl mercury does not depend on sulfate reduction can indicate that there is limited inorganic mercury available for methylation or that iron reducing bacteria (FeRB) could be the primary methylators of mercury (Mitchell and Gilmour, 2008[b]).

Microbial and Geochemical Controls on MeHg production

In the St. Louis River estuary, evidence suggests that there are different factors limiting sediment MeHg production in each site. Organic carbon can influence the production in MeHg via two separate mechanisms. A lack of labile organic carbon can limit the production of methyl mercury by limiting the microbial activity of SRB in sediments (Lambertsson et al. 2006). Organic carbon can also limit the bioavailability of inorganic mercury to SRB, thereby decreasing mercury methylation (Hammerschmidt and Fitzgerald 2004[a]). Both carbon related MeHg limiting process appear to be occurring in the St. Louis River Estuary sediment, depending on the habitat zone. In the LEF habitat zone, organic carbon in the sediment is refractory (high C/N ratio, Figure 4). Figure 18 depicts a significant ($p < 0.05$) negative correlation between total carbon and %MeHg in the LEF system, similar to the trend observed by Hammerschmidt and Fitzgerald (2004[a]). Since the organic carbon supplied to the LEF habitat zone is refractory, organic carbon at this site may bind inorganic mercury (thus limiting the supply of bioavailable inorganic mercury) while not providing the energy to drive methylating microbial processes. The net effect of carbon in LEF sediment, therefore would be a lower in production of MeHg.

The second organic carbon limiting mechanism is proposed for the SB and UEF habitat zones. A significant relationship between organic carbon and %MeHg ($p < 0.05$) was observed in the SB habitat zone (Figure 18) but was not significant ($p > 0.05$) for the UEF sediment. Since the organic carbon supplied in the UEF and SB habitat zones in not as recalcitrant, it may function as a ligand for inorganic mercury but also drive microbial activity. Both UEF and SB sediment had much lower porewater total mercury than LEF (2.3x and 6x smaller, respectively), but consistently higher %MeHg. Despite having porewater total mercury concentrations 2-3x lower than UEF, SB had similar %MeHg, possibly due to greater overall activity of sulfate reduction driven by a larger quantity of carbon.

Many studies have cited a limitation of inorganic mercury available for methylation due to high porewater sulfide concentrations (Benoit et al. 1999[a]; Benoit, 2003; Gilmour et al. 1998). Additionally, transport of MeHg from sediments is believed to be accelerated in the presence of dissolved sulfide (Berndt and Bavin, 2011; Jonsson et al. 2010). In the St. Louis River estuary, sulfide concentrations were uniformly below the detection limit (1-5uM), which is below the proposed threshold of sulfide limitations on MeHg production (<5-10 uM sulfide, Benoit, 2003); however, it is possible that iron sulfides may be limiting the bioavailability of inorganic mercury to SRB by binding it to the solid phase (Bower et al. 2008; Liu et al 2009). The sulfide concentration at which inorganic- and methyl- mercury speciation shifts from organic ligands to sulfide ligands is dependent upon the sulfur content of organic carbon (Skyllberg 2008) which is not known for the St. Louis River Estuary. However, the low sulfide conditions observed in the estuary would likely favor organic carbon as a ligand relative to sulfidic environments encountered elsewhere in the St. Louis watershed (Berndt and Bavin, 2011).

Porewater Mercury Partitioning Coefficients and Flux Estimates

Porewater total- and methyl- mercury was measured in bulk sediment from the top 10cm in each of the microcosms at the close of the experiments (Tables 1 and 2). No discernible trend was observed for porewater THg or MeHg among high, medium, and low sulfate treatments, and values from each habitat zone are averaged for analysis. Porewater total mercury concentrations appeared to be strongly related to the total organic carbon at the three study sites, with SB having the lowest concentrations (4.5±1.8 ng/L), UEF having higher porewater THg (12.3±5.4 ng/L), and LEF having the highest porewater THg concentrations (26.3±21.6 ng/L). Porewater methyl mercury was less variable, with all sites averaging between 0.32 and 0.46 ng/L. Sediment from the LEF habitat zone had the most variable solid-phase and dissolved-phase total- and methyl- mercury concentrations.

Partitioning coefficients for THg and MeHg are presented in Tables 1 and 2 for each habitat zone. For THg, the UEF and LEF have the lowest log K_D values of 3.9±0.1 and 3.9±0.2, respectively, while the SB had the largest log K_D value of 4.70±0.2. The lower total mercury log K_D values for LEF and UEF may be due to lower TC values relative to the SB sediment. TC and K_D tend to be positively correlated since THg sorbs strongly to organic matter (Hammerschmidt and Fitzgerald 2004[a]).

MeHg partitioning coefficients are all fairly similar among habitat zones with the UEF habitat zone having the lowest K_D value (3.2±0.5) relative to the SB (3.6±0.1) and LEF (3.4±0.5) habitat zones. In addition to inorganic mercury, organic carbon also binds MeHg very strongly and may be controlling the partitioning of MeHg to the solid phase (SB had highest K_D for both THg and MeHg). Sulfide concentrations remained low (<5uM) in all estuary sediment, potentially resulting in

conditions that favor organic ligands over sulfide in MeHg speciation (Dryssen and Wedborg 1991).

THg flux measurements to the overlying water made at the close of lab experiments are summarized in Table 2 for each habitat zone. The change in mass of mercury in the overlying water over a 36-48 hour time period was normalized for surface area according to Equation 1.

$$Flux_{Hg} = \frac{\Delta C \cdot V_W}{\Delta t \cdot A} \qquad \text{Equation 1}$$

Where

- ΔC is the change in overlying water mercury concentration
- V_W is the volume of the overlying water
- Δt is the time of the flux experiment, and
- A is the surface area of the sediment microcosm.

Consistent with porewater measurements, no discernible trend was observed in flux measurements among high, medium, and low sulfate treatments, so results were averaged for each habitat zone. THg flux out of the St. Louis River Estuary habitat zones was between 15 and 38 ng/m2/d (Table 1), and is in agreement with estimated fluxes from other sediment systems (Gill et al. 1999[a]). THg flux out of the sediment, similar to porewater concentrations, seems to be influenced by organic carbon with SB and UEF having the lowest flux (15.5 and 18.5 ng/m2/day, respectively), and LEF having the highest flux (38 ng/m2/day). Since the LEF and UEF habitat zones have similar Log(KD) values, larger solid phase THg concentrations appear to be driving larger fluxes in the LEF habitat zone (Table 1).

MeHg flux was measured in the sediment microcosms, but differences between initial and final MeHg were not adequate to calculate fluxes. In order to estimate MeHg fluxes, the net mass transfer resistance (effective diffusion) observed in total mercury flux experiments was employed. Flux across the sediment water interface can be given by:

$$F\left[\frac{ng}{cm^2 - day}\right] = k_{mt}\left[\frac{cm}{day}\right]\left(C_{pw} - C_{overlying}\right)\left[\frac{ng}{cm^3}\right] \qquad \text{Equation 2}$$

Since THg flux, overlying water concentration, and porewater concentration are known for THg experiments, an effective mass transfer coefficient (kmt) can be calculated for each THg flux experiment. MeHg flux was estimated by assuming that mass transfer resistances for MeHg are similar to that of THg. Mass transfer coefficients for the three sulfate treatments in each habitat zone were then averaged and used in MeHg flux calculations according to Equation 2. Calculated MeHg flux values for the LEF, UEF, and SB habitat zones are displayed in Table 3 and are in agreement in magnitude with those estimated in the Long Island Sound (CT) system

(Hammershmidt et al 2004[b]). The SB, having the largest kmt, has the largest MeHg flux value (1.68 ng m-2 hr-1) while the UEF and LEF have lower values of 0.45 and 0.79 ng m-2 hr-1, respectively.

Experiments utilizing sediment from each habitat zone was scaled to the total area of the Habitat zone within the estuary. MeHg flux values and areas were used to calculate sediment MeHg loading (ng hr-1) to the St. Louis River Estuary (Table 3). MeHg loading from the upstream St. Louis River (Figure 3) was calculated using MeHg concentrations measured by Berndt and Bavin (2009 and 2012) and discharges from USGS gauge stations located at the Scanlon Dam at multiple time points (St. Louis River discharges were taken from the same day MeHg water samples were obtained). The estimated MeHg loads from the UEF, LEF, and SB habitat zones were 3.70, 8.31, and 6.05 mg hr-1, respectively. The incoming MeHg load at the Scanlon Dam was calculated to be 7.22 mg hr-1 during low flow conditions and 336.4 during high flow conditions (Table 4). Median flow conditions (around 28000 L s-1) carried a MeHg load of 15.29 mg hr-1 from upstream sources. If summed, the total MeHg load from the three habitat zones examined in this study (representing 45% of the total area in the St. Louis River Estuary) exceeds that being delivered from upstream sources during both median and low flow conditions. These numbers suggest that production and transport of MeHg from sediments represents a significant portion of MeHg delivered to the St. Louis River (Table 4) during normal and low flow conditions. During the spring, when streamflow is at its annual high, MeHg contribution from sediment is a much smaller fraction relative to upstream MeHg loads. Understanding the magnitude of MeHg flux from sediments in the estuary will help to inform watershed managers whether active management to control MeHg production and flux from estuary sediments is necessary.

5. Conclusions and Implications

Results from the sulfate addition experiments suggest that MeHg production in sediment of the St. Louis River Estuary was largely controlled by carbon except in one case when sulfate in the overlying water appeared to be important. Over the timescale of these experiments (6 months), no habitat zones exhibited a significant change in sediment %MeHg in the surficial sediment (0-4cm) as a result increased or decreased sulfate in the overlying water. However, measurements in the LEF habitat zone showed that %MeHg in deeper sediments (4-10cm) appeared to be related to sulfate in the overlying water (Figures 12-14).

Carbon controls on MeHg production in each habitat zone was related to the type and quantity of carbon present. In the SB habitat zone, large quantities of organic carbon and iron sulfides (represented by AVS) are likely limiting the amount of inorganic mercury available to microbial communities for methylation. The UEF and SB had similarly low C/N ratios which

could drive higher microbial activity (Figure 4); however lower total carbon in the UEF may be the cause of higher porewater inorganic mercury (relative to the SB sediment) available for methylation and transport (Table 1). Since the UEF is the only habitat zone which does not display a positive significant correlation between %MeHg and SRB abundance (Figure 17), FeRB may play an important role in the production of MeHg. It should be noted that the %MeHg in the 0-4 cm depth of the UEF low sulfate treatment (Figure 14) appears to be an outlier (Figure 17 and Figure 18) and calls into question the significance of the higher %MeHg observed in response to a decrease in overlying water sulfate.

The Sheltered Bay (SB) and Upper Estuary Flats (UEF) habitat zones initially were the most efficient methylators of mercury, with %MeHg values (0.8-1.3 %MeHg) similar to those found in other aquatic systems (Kim et al. 2011). The UEF site had the highest %MeHg possibly due to two factors: low log K_D (3.9 ± 0.13) indicating significant porewater concentrations; and low C/N ratio (15.9 ±2.1 C/N) indicating availability of labile organic carbon. Both the UEF and SB habitat zones, according to the data presented, may be limited in the mercury methylation process by porewater bioavailable inorganic mercury, not sulfate. Although strong associations with organic carbon may limit MeHg production in the high organic SB habitat zone, significant flux was still observed as indicated by the high effective diffusion (mass transfer) coefficient (Tables 1 and 3).

Another conclusion from the data presented is that decreasing sediment THg concentrations could result in a decrease in MeHg production (Figure 16). It has been observed in both the dataset presented here for the St. Louis Estuary and in the literature (Benoit et al. 2003) that MeHg concentrations are strongly related to THg concentrations in sediment that is not highly contaminated by mercury (<500 ng/g). In all sites for this study, there was a significant positive relationship between THg and MeHg. Although scientifically answering the question of sulfate and carbon limitations to sediment MeHg production and transport could help to evaluate management alternatives, decreasing atmospheric and terrestrial mercury loading to the St. Louis River Estuary could lead to an decrease in sediment MeHg concentrations.

MeHg and THg flux was estimated for each habitat zone to quantify the mass loadings of mercury to the St. Louis River Estuary System. It was calculated that the three habitat zones examined in this study (44.9% of the entire estuary area) could contribute a MeHg load of 18.1 mg hr-1 from sediment while the upstream contribution discharging into the estuary is 15.3 mg hr-1 during median stream flow and 7.2 mg hr-1 during low flow conditions. Although the residence time of the estuary is not well known to support a complete mass balance, these calculations indicate that sediment contributions may play a significant role in defining MeHg concentrations in the overlying water.

This study answered multiple scientific and management questions related to the production and transport of MeHg in the St. Louis River Estuary. The first question answered was whether changing sulfate concentrations in the overlying water would influence MeHg concentration in sediments in light of the various factors limiting MeHg production in each habitat zone. From a management standpoint, results suggest that sediment loading contributes a significant amount of inorganic and methyl mercury to the water column, relative to upstream loading. This revelation implies that MeHg production and transport processes in sediments should be accounted for when considering the total pool of MeHg in the St. Louis River Estuary. Although further investigation of sediment-related mercury dynamics and hydrodynamic mixing in the St. Louis River Estuary will be necessary to achieve a full mass balance for MeHg, the results presented here have illuminated the role of sulfate on the production and transport of MeHg in the St. Louis River Estuary sediment.

6. References

Benoit, J.M., Gilmour C.C., Mason, R.P., Heyes, A. (1999a). Sulfide Controls on Mercury Speciation and Bioavailability to Methylating Bacteria in Sediment Pore Waters. Environmental Science and Technology 33(6): 951-957.

Benoit, J.M., Mason, R.P., Gilmour, C.C. (1999b). Estimation of mercury sulfide-speciation in sediment pore waters using octanol-water partitioning and implications for availability to methylating bacteria. Environmental Toxicology and Chemistry 18(10): 2138-2141.

Benoit, J.M., Gilmour C.C., Mason, R.P. (2001). Aspects of Bioavailability of Mercury for Methylation in pure cultures of *Desulfobulbus propionicus* (1pr3). Applied and Environmental Microbiology 67(1): 51-58.

Benoit, J.M., C.C., Gilmour, Heyes, A., Mason, R.P., Miller, C.L. (2003). Geochemical and biological controls over methylmercury production and degredation in aquatic ecosystems. Biogeochemistry of Environmentally Important Trace Elements – ACS Symposium Series 835: 262-297.

Benoit, J. M., Shull, D. H., Harvey, R. M., and Beal, S. A. (2009) Effect of Bioirrigation on Sediment-Water Exchange of Methylmercury in Boston Harbor, Massachusetts. Environmental Science and Technology 43(10): 3669-3674.

Berndt, M., and Bavin, T. (2009) Sulfate and Mercury Chemistry of the St. Louis River in Northeastern Minnesota. Report to the Minerals Coordinating Committee. 12/15/2009.

Berndt, M., and Bavin, T. (2011) Sulfate and Mercury Cycling in Five Wetlands and a Lake Receiving Sulfate from Taconite Mines in Northeastern Minnesota. Minnesota Department of Natural Resources, Divison of Lands and Minerals. 12/15/2011.

Berndt, M., and Bavin, T. (2012) Personal communication. Regarding recent (spring 2012) mercury data collected at the St. Louis at Cloquet (unpublished). 7/19/12.

Bower, J., Savage, K.S., Weinman, B., Barnet, M.O., Hamilton, W.P., Harper, W.F. (2008). Immobilization of mercury by pyrite (FeS2). Environmental Pollution. 156(2): 504-514.

Branfireun, B.A., Roulet, N.T., et al. (1999). In situ sulfate stimulation of mercury methylation in a boreal peatland: Toward a link between acid rain and methylmercury contamination in remote environments. Global Geochemical Cycles 13(3): 743-750.

Brendel, P.J. and Luther, G.W. (1995). Development of a gold amalgam voltammetric microelectrode for the determination of dissolved Fe, Mn, O2, and S(-II) in porewaters of marine and fresh-water sediments. Environmental Science and Technology 29(3): 751-761.

Brouwer, H. and Murphy, T.P. (1994). Diffusion method for the dermination of acid-volatile sulfides (AVS) in sediment. Environmental Toxicology and Chemistry 13(8): 1273-1275.

Brown, E.T., Laurence, L.C., et al. (2000). Geochemical cycling of redox sensitive metals in sediments from lake Malawi: a diagnostic paleotracer of episodic changes in mixing depth. Geochimica et Cosmochimica Acta 64(20): 3515-3523.

Choe, K.Y., Gill, G.A., Lehman, R.D., Seunghee, H., Heim, W.A., Coale, K.H. (2004). Sediment-Water Exchange of Total Mercury and Monomethylmercury in the San Francisco Bay Delta. Limnology and Oceanography 49(5): 1512-1527.

Coleman Wasik, J. K., Mitchell, C. P. J., Engstrom, D. R., Swain, E. B., Monson, B. A., Balogh, S., J., Jeremiason, J. D., Branfireun, B., A., Eggert, S. L., Kolka, R. A., and Almendinger, J. E. (2012) Methylmercury Declines in a Boreal Peatland When Eperimental Sulfate Deposition Decreases. Environmental Science and Technology 46(12): 6663-6671.

Compeau, G.C. and Bartha, R. (1985). Sulfate-Reducing Bacteria: Principal Methylators of Mercury in Anoic Estuarine Sediment. Applied and Environmental Microbiology 50(2): 498-502.

Covelli, S, Faganeli, J., Hovart, M., and Brambati, A. (1999) Porewater Distribution and Benthic Flux Measurements of Mercury and Methylmercury in the Gulf of Trieste (Northern Adriatic Sea). Estuarine, Coastal and Shelf Science 48(4):415-428.

Covelli, S; Faganeli, J.; De Vittor, C.; Predonzani, S.; Acquavita, A.; Horvat, M. (2008) Benthic fluxes of mercury species in a lagoon environment (Gradoo Lagoon, Northrn Adriatic Sea, Italy). Applied Geochemistry (23)529–546.

Crane, J.L. (2006) Sediment Quality Conditions in the Lower St. Louis River, Minnesota/Wisconsin. MPCA Document Number: tdr-fg05-04

DiPasquale, M. M., Agee, J., McGowan, C., Oremland, R. S., Thomas, M., Krabbenhoft, D., and Gilmour, C. C. (2000). Methyl-Mercury Degradation Pathways: A Comparison among Three Mercury-Impacted Ecosystems. Environmental Science and Technology. 34(23): 4908–4916

Drott, A., Lambertsson, L., Bjorn, E., Skyllberg, U. (2007). Importance of dissolved neutral mercury sulfides for methylmercury production in contaminated sediments. Environmental Science and Technology 41(7): 2270-2276.

Drott, A., Lambertsson, L., et al. (2008). Do potential methylation rates reflect accumulated methylmercury in contaminated sediments? Environmental Science and Technology 42(1): 153-158.

Dyrssen, D., Wedborg, M. (1991) The Sulfur-Mercury(II) System in Natural-Waters. Water, Air, Soil Pollution 56: 507-519.

Eaton, D.A., Clesceri, L.S., et al. (2005). Standard Methods for the Eamination of Water & Wastewater – 4500-S^{2-} G. Ion-Selective Electrode Method. American Public Health Association.

Fitzgerald, W.F., Engstrom, D.R., Mason, R.P., Nater, E.A.. (1998). The case for atmospheric mercury contamination in remote areas. Environmental Science and Technology 32(1): 1-7.

Fitzgerald, W. F., C. H. Lamborg, et al. (2007). Marine biogeochemical cycling of mercury. Chemical Reviews 107(2): 641-662.

Flemming, E.J., Mack, E.E., et al. (2006). Mercury Methylation from Unexpected Sources: Molybdate-Inhibited Freshwater Sediments and an Iron-Reducing Bacterium. Applied and Environmental Microbiology 72(1): 457-464.

Fossing. H., Berg, P., et al. (2004). A model set-up for an oygen and nutrient flux model for Aarhus Bay (Denmark). National Environmental Research Institute.

Froelich, G.P., Klinkhammer, M.L., Bender, N.A., Luedtke, G.R., Cullen, D., Daulphin, P., Hammond, D., Blayne H., Maynard, V. (1978). Early oxidation of organic matter in pelagic sediments of the eastern equatorial Atlantic: suboic diagenesis. Geochimica et Cosmochimica Acta 43(7): 1075-1090.

Gill, G.A., Bloom, N.S., Cappellino, S., Driscoll, C.T., Dobbs, C., McShea, L., Mason, R., Rudd., J.W.M. (1999a). Sediment-Water Fluxes of Mercury in Lavaca Bay, Teas. Environmental Science and Technology. 33(5): 663-669.

Gilmour, C.C., Henry, E.A., Mitchell, R. (1992). Sulfate Stimulation of Mercury Methylation in Fresh-Water Sediments. Environmental Science and Technology 26(11): 2281-2287.

Gilmour, C.C., Riedel, G.S., Ederington, M.C., Bell, J.T., Benoit, J.M., Gill, G.A., Stordal, M.C. (1998). Methylmercury concentrations and production rates across a trophic gradient in the northern Everglades. Biogeochemistry 40(2-3): 217-345.

Golding, G.R., Kelly, C.A., Sparling, R., Loewen, P.C., Rudd, J.W.M., Barkay, T. (2002). Evidence for facilitated uptake of Hg(II) by *Vibrio anguillarum* and *Escherichia coli* under anaerobic and aerobic conditions. Limnology and Oceanography 47(4): 967-975.

Graham, A.M., Aiken, G.R., Gilmour, C.C. (2012). Dissolved Organic Matter Enhances Microbial Mercury Methylation under Sulfidic Conditions. Environmental Science and Technology 46(5): 2715-2723.

Gray, J.E., and Hines, M.E., (2009). Biogeochemical mercury methylation influenced by reservoir eutrophication, Salmon Falls Creek Reservoir, Idaho, USA. Chemical Geology 258, 157-167.

Hammerschmidt, C.R. and Fitzgerald, W.F. (2004). Geochemical Controls on the production and distribution of methylmercury in near-shore marine sediments. Environmental Science and Technology 38(5): 1487-1495.

Hammerschmidt, C.R., Fitzgerald, W.F., Lamborg, C.H., Balcom. P.H., Visscher., P.T.. (2004b). Biogeochemistry of methylmercury in sediments of Long Island Sound. Marine Chemistry 90(1-4): 31-52.

Hammerschmidt, C. R. and Fitzgerald, W.F. (2008a) Sediment-water echange of methylmercury determined from shipboard benthic flu chambers. Marine Chemistry 109(1-2): 86–97.

Hammerschmidt, C. R.; Fitzgerald,W.F.; Balcom, P. H.; Visscher, P. T.(2008b) Organic matter and sulfide inhibit methymercury production in sediments of New York/New Jersey Harbor. Marine Chemistry 109(1-2): 165–182.

Harmon, S.M., King, J.K., Gladden, J.B., Chandler, G.T., Newman, L.A. (2004). Methylmercury Formation in a Wetland Mesocosm Amended with Sulfate. Environmental Science and Technology 38(2): 650-656.

Harmon, S.M. King, J.K., Gladden, J.B., Newman, L.A. (2007). Using sulfate-amended slurry batch reactors to evaluate mercury methylation. Archives of Environmental Contamination and Toxicology 52(3): 326-331.

Hicks, R.E. and Oster, R.J. (2012). Developing a Risk Assessment Tool to Predict the Risk of Accelerated Corrosion to Port Infrastructure. Great Lakes Maritime Research Institute 1-20.

Hintelmann, H. and Evans, R.D. (1997). Application of stable isotopes in environmental tracer studies – Measurement of monomethylmercury (CH3Hg+) by isotope dilution ICP-MS and detection of Species transformation. Fresenius Journal of Analytical Chemistry 358(2): 378-385.

Hintelmann, H. and Ogrinc, N. (2003). Determination of Stable Mercury Isotopes by ICP/MS and Their Applications in Environmental Studies. Biogeochemistry of Environmentally Important Trace Elements – ACS Symposium Series 835: 321-338.

Horvat, M., Bloom, N.S., Liang., L. (1993). Comparison of distillation with other current isolation methods for determination of methylmercury compounds in low level environmental samples. Analytica Chimica Acta 281(1): 135-152.

Jeremiason, J.D., Engstrom, D.R., Swain, E.B., Nater, E.A., Johnson, B.M., Almendinger, J.E., Monson, B.A., Kolka, K.A. (2006). Sulfate Addition Increases Methylmercury Production in an Experimental Wetland. Environmental Science and Technology 40(12): 3800-3806.

Johnson, N.W., Reible, D.D., Katz. L. E. (2010) Biogeochemical Changes and Mercury Methylation beneath an In-Situ Sediment Cap. Environmental Science and Technology 44(19): 7280-7286.

Johnson, N. W. and Beck, B. (2011) The Role of Sulfate Reduction in the St. Louis River Estuary. NIWR Annual Technical Report.

Jonsson, S., Skyllberg, U., Bjorn, E. (2010). Substantial Emission of Gaseous Monomethylmercury from Contaminated Water-Sediment Microcosms. Environmental Science and Technology. 44(1):278-283.

Jorgensen, B.B. (1982). Mineralization of organic matter in the sea bed-the role of sulphate reduction. Nature 296(5858): 643-645.

Katsev, S., Sundby, B., Mucci, A. (2006). Modeling vertical excursions of the redox boundary in sediments: Application to deep basins of the Arctic Ocean. Limnology and Oceanography 51(4): 1581-1593.

Kerin, E.J., Gilmour, C.C., Roden, E., Suzuki, M.T., Coates, J.D., Mason, R.P. (2006). Mercury methylation by dissimilatory iron reducing bacteria. Applied and Environmental Microbiology 72(12): 7919-7921.

Kim, M., Han, S., Gieskes, J., Deheyn, D.D. (2011). Importance of organic matter lability for monomethylmercury production in sulfate-rich marine sediments. Science of the Total Environment 409(4): 778-784.

King, J.K., Saunders, F.M., Lee, R.F., Jahnke, R.A.. (1999). Coupling mercury methylation rates to sulfate reduction rates in marine sediments. Environmental Toxicology and Chemistry 18(7): 1362-1369.

King, J.K., Kostka, J.E., Frischer, M.E., Saunders, F.M. (2000). Sulfate reducing bacteria methylate mercury at variable rates in pure culture and in marine sediments. Applied and Environmetal Microbiology 66(6): 2430-2437.

Liu, J., Valsaraj K. T., Delaune., R.D. (2009). Inhibition of Mercury Methylation by Iron Sulfides in Anoxic Sediment. Environmental Engineering Science 26(4): 833-840.

Lambertsson, L. and Nilsson, M. (2006). Organic material: The Primary Control on mercury methylation and ambient methylmercury concentrations in estuarine sediments. Environmental Science and Technology 40(6): 1822-1829.

Meyers, P.A. and Ishiwatari, R. (1993). Lacustrine Organic Geochemistry – An Overview of Indicators of Organic Matter Sources and diagenesis in Lake Sediments. Organic Geochemistry 20(7): 867-900.

Mitchell, C.J., Branfireun, B.A., Kolka, K. K. (2008a). Assessing sulfate and carbon controls on net methylmercury production in peatlands: An in situ mesocosm approach. Applied Geochemistry 23(3): 503-518.

Mitchell, C.J. and Gilmour, C.C. (2008b). Methylmercury production in a Chesapeake Bay Salt Marsh. Journal of Geophysical Research 113: 1-14.

Phillips, E.J., Lovely, D.R. (1987). Determination of iron(III) and iron(II) in oxalate extracts of sediment. Soil Science Society of America Journal 51(4): 938-941.

Ratcliffe, H.E., Swanson, G.M., Fischer, L.J. (1996). Human eposure to mercury: a critical assessment of the evidence of adverse health effects. Journal of Toxicology and Environmental Heath 49(3): 221-270.

Schaefer, J.K. and Morel., F.M. (2009). High methylation rates of mercury bound to cysteine by *Geobacter sulfurreducens.* Nature Geoscience 2(2): 123-126.

Schaefer, J.K., Rocks, S.S., Zheng, W., Liang, L.Y., Gu, B.H., Morel, F.M. (2011). Active transport, substrate specificity, and methylation of Hg(II) in anaerobic bacteria. Proceedings of the National Academy of Sciences of the United States of America 108(21): 8714-8719.

Schippers, A. and Neretin, L.N. (2006). Quantification of microbial communities in near surface and deeply buried sediments on Peru continental margin using real-time-PCR. Environmental Microbiology 8: 1251-1260.

Sellers, P., Kelly, C.A., Rudd, J.W.M., MacHutchon, A.R. (1996). Photodegradation of methylmercury in lakes. Nature 380(6576): 694-697.

Skyllberg, U., Bloom, P. R., Qian, J., Lin, C. M., Bleam, W. F. (2006) Complexation of Mercury(II) in Soil Organic Matter: EAFS Evidence for Linear Two-Coordination with Reduced Sulfur Groups. Environmental Science and Technology 40(13): 4174-4180.

Skyllberg, U. (2008). Competition among thiols and polysulfides for Hg and MeHg in wetland soils and sediments under suboic conditions: Illuminations of controversies and implications for MeHg net production. Journal of Geophysical Research-Biogeosciences 113: 1-14.

Skyllberg, U. and Drott, A. (2010). Competition between Disordered Iron Sulfide and Natural Organic Matter Associated Thiols for Mercury(II)-An EXAFS study. Environmental Science and Technology 44(4): 1254-1259.

St Louis River Allinace (SLRA). (2002). Lower St. Louis River Habitat Plan. St. Louis River Alliance, Duluth, MN. http://www.stlouisriver.org/.

Stumm, W. and Morgan, J.J. (1996) "Aquatic Chemistry, Chemical Equilibria and Rates in Natural Waters." Wiley & Sons.

Todarova, S.G., Driscoll, C.T., Matthews, D.A., Effler, S.W., Hines, M.E., Henry, E.A . (2009). Evidence for Regulation of Monomethyl Mercury by Nitrate in a Seasonally Stratified, Eutrophic Lake. Environmental Science and Technology 43(17): 6572-6578.

Vannote, R.L., Minshall ,G.W., Cummins, K.W., Sedell, J.R., Cushing, C.E. (1980). The River continuum concept. Canadian Journal of Fisheries and Aquatic Sciences 37(1): 130.

Wetzel, R.G. (2002). Limnology, Third Edition: Lake and River Ecosystems. Elesvier Science.

WI DNR (Wisconsin Department of Natural Resources) (2011). Fish Consumption Advice for the St. Louis River Area of Concern. http://dnr.wi.gov/topic/fishing/eatyourcatch.html.

Acknowledgements

This study was funded jointly by the Minnesota Environment and Natural Resources Trust Fund as recommended by the Legislative-Citizen Commission on Minnesota Resources (LCCMR) and the USGS's State Water Resources Research Institute program run through the Minnesota Water Resources Center.

The authors of this report would like to thank several others who contributed intellectually or through sample analysis: Carl Mitchell, Dan Engstrom, Michael Berndt, Ed Swain, Randall Hicks, Amanda Brennan, and Ryan Oster.

Figures & Tables

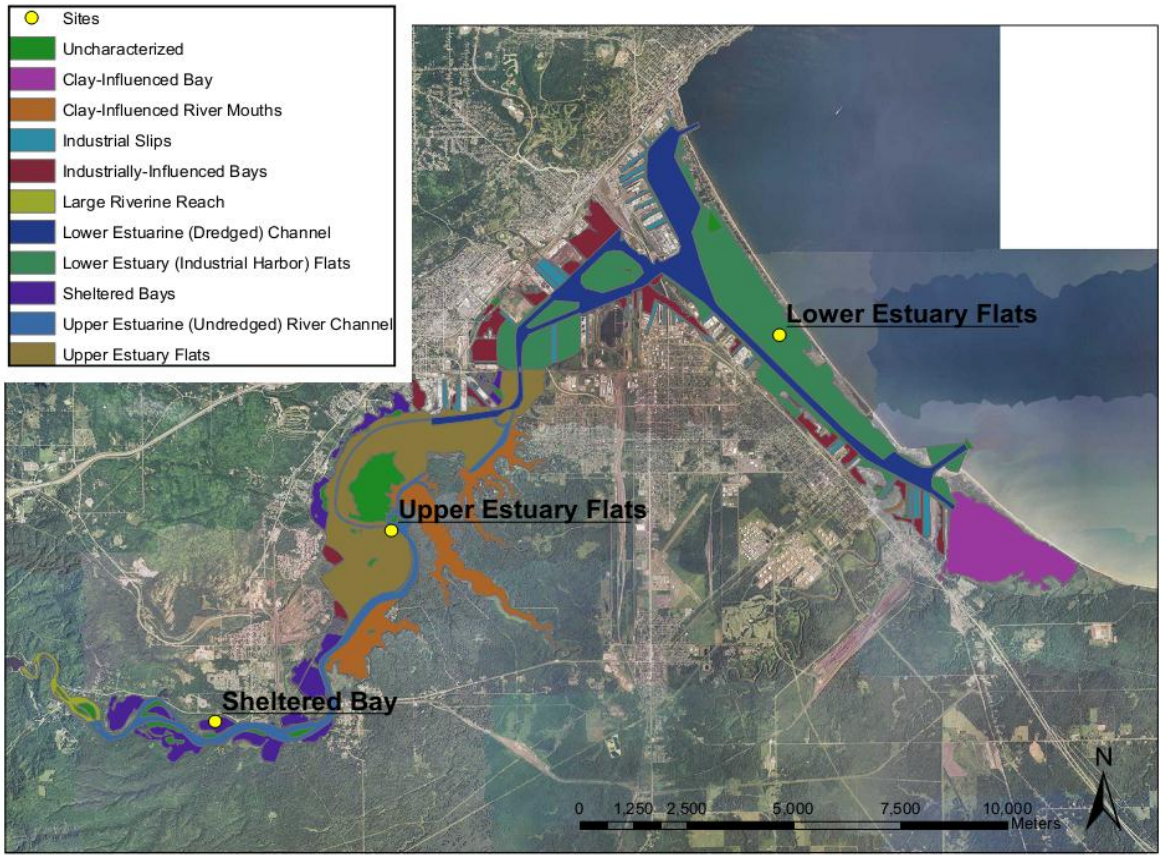

Figure 1. St. Louis River Estuary with Habitat Zones delineated by the SLRA. Sites sampled in August 2011 are highlighted in yellow.

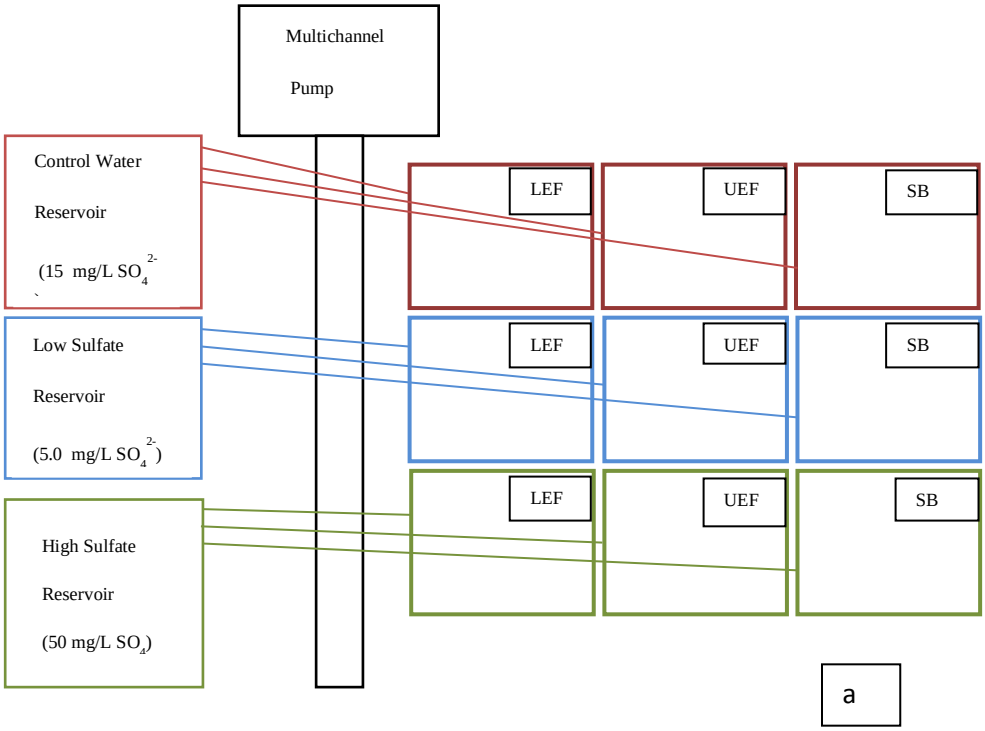

Figure 2. Schematic of experimental design including treatment concentrations (a) and a photo of the experimental setup within the temperature control chamber (b).

Figure 3. Sediment Core tube attached to sediment corer and drive rod. Ball valves displayed in an open position, which was used when driving core tube into sediment and closed 90º when core had reached its desired depth.

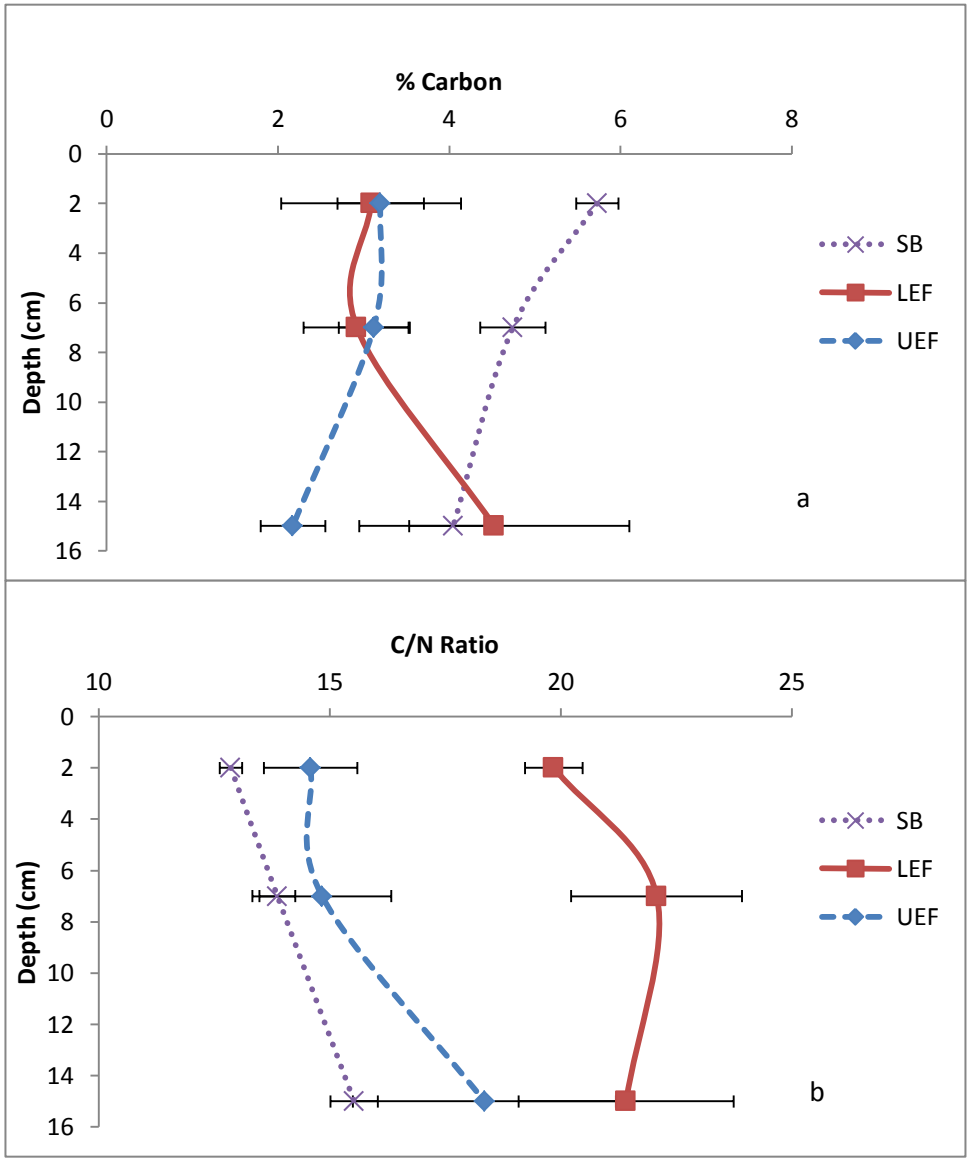

Figure 4. Total Carbon (TC) (a) and C/N ratio (b) sediment profiles. Sediment profiles were averaged for each site since TC and C/N ratios went unchanged during the experiment time period.

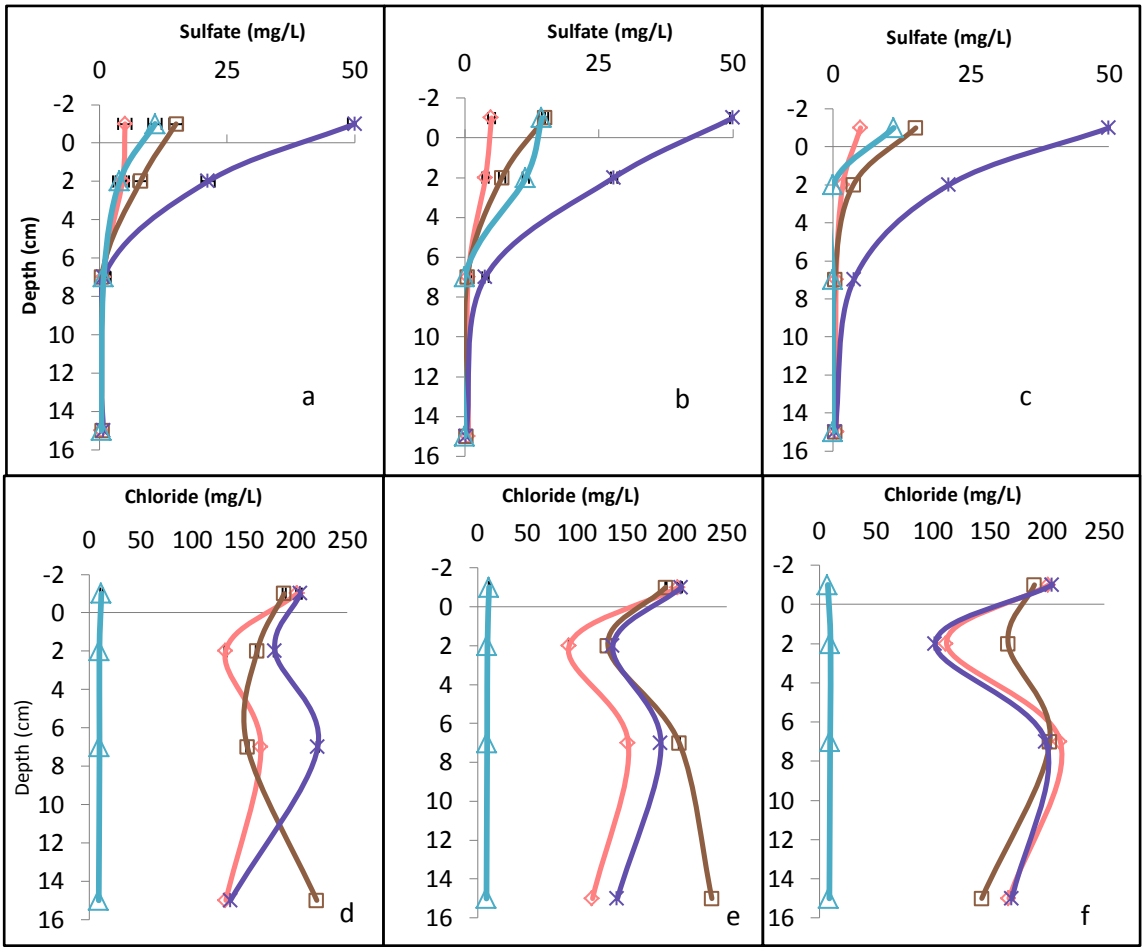

Figure 5. Sulfate and chloride sediment profiles for UEF (a and d), LEF, (b and e), and SB(c and f) sites including overlying water concentrations for high (purple crosses), low (pink diamonds), medium (brown squares), and initial profiles (blue triangles).

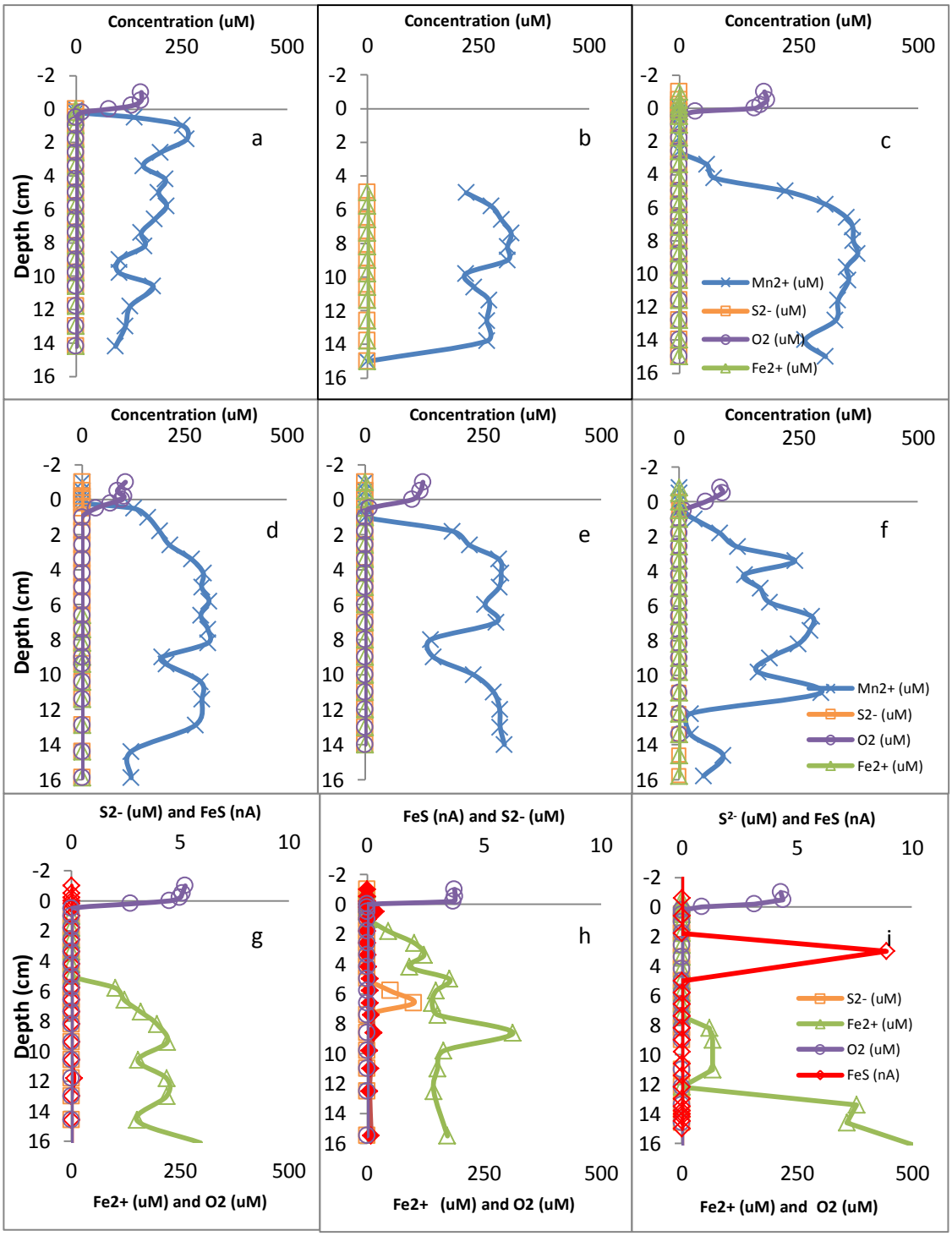

Figure 6. Initial condition porewater redox profiles for the LEF (low (a), medium (b), high(c)), UEF (low(d), medium(e), and high(f)), and SB (low (g), medium (h), and high(i)) experiments.

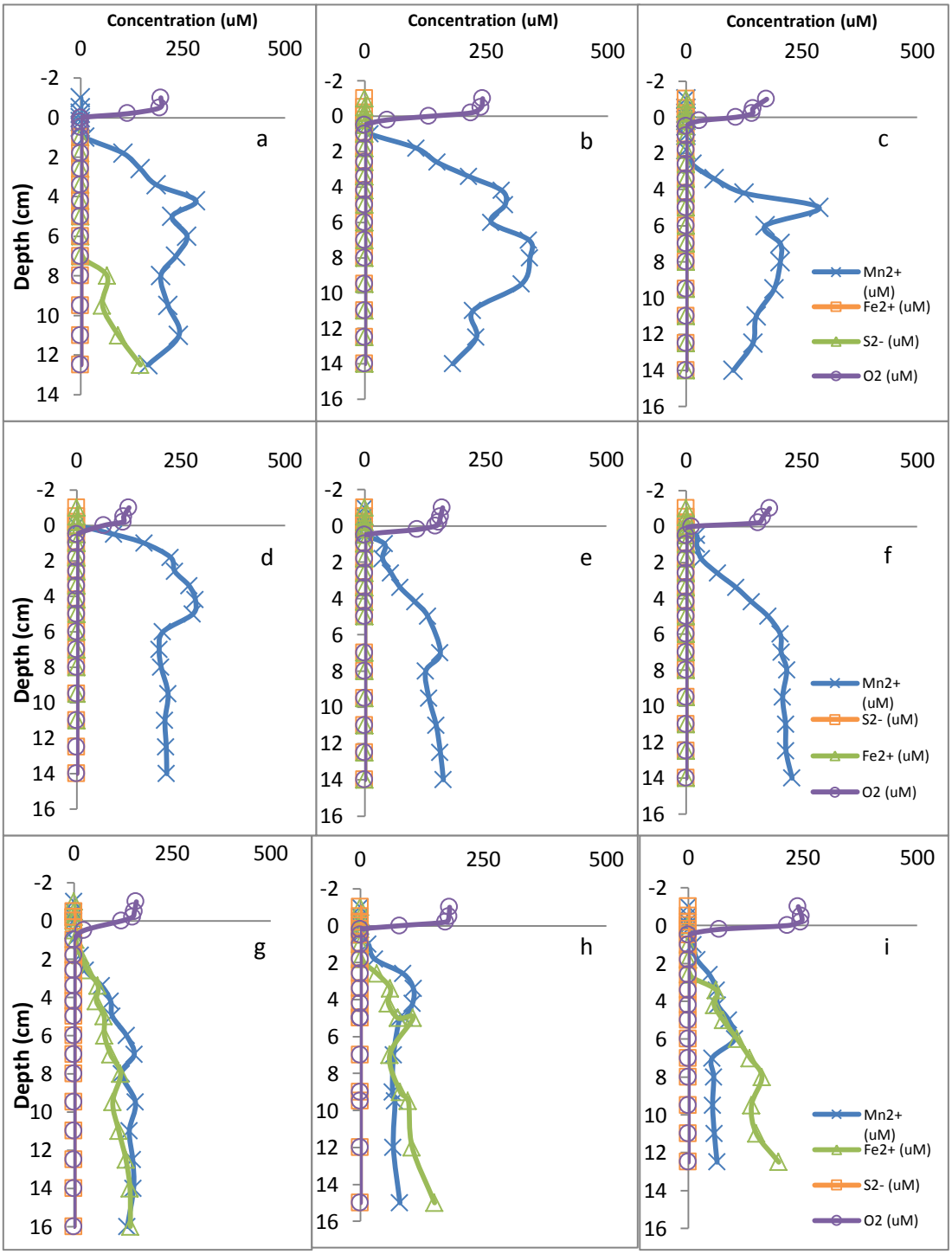

Figure 7. Final condition porewater redox profiles for the LEF (low (a), medium (b), high(c)), UEF (low(d), medium(e), and high(f)), and SB (low (g), medium (h), and high(i)). FeS was not added to this figure since there was no detectable FeS in any of the microcosms.

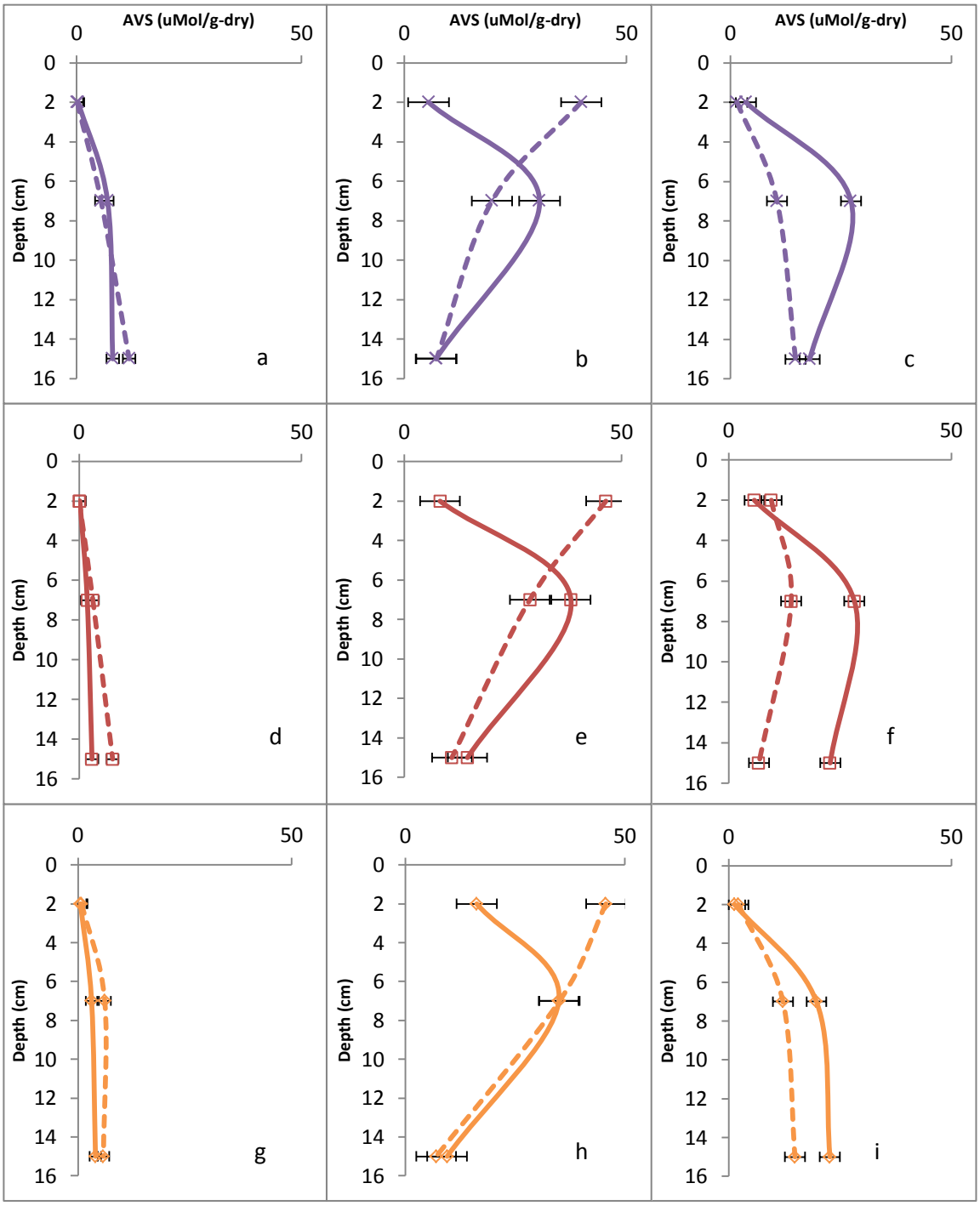

Figure 8. Sediment AVS profiles of Initial (dotted lines) and final (solid lines) for LEF (a, d, and g), SB (b, e, and h), and UEF (c, f, and i). High sulfate treatments (a-c) are displayed in purple crosses, medium treatments (d-f) are displayed in red squares and low treatments (g-i) are displayed in yellow diamonds.

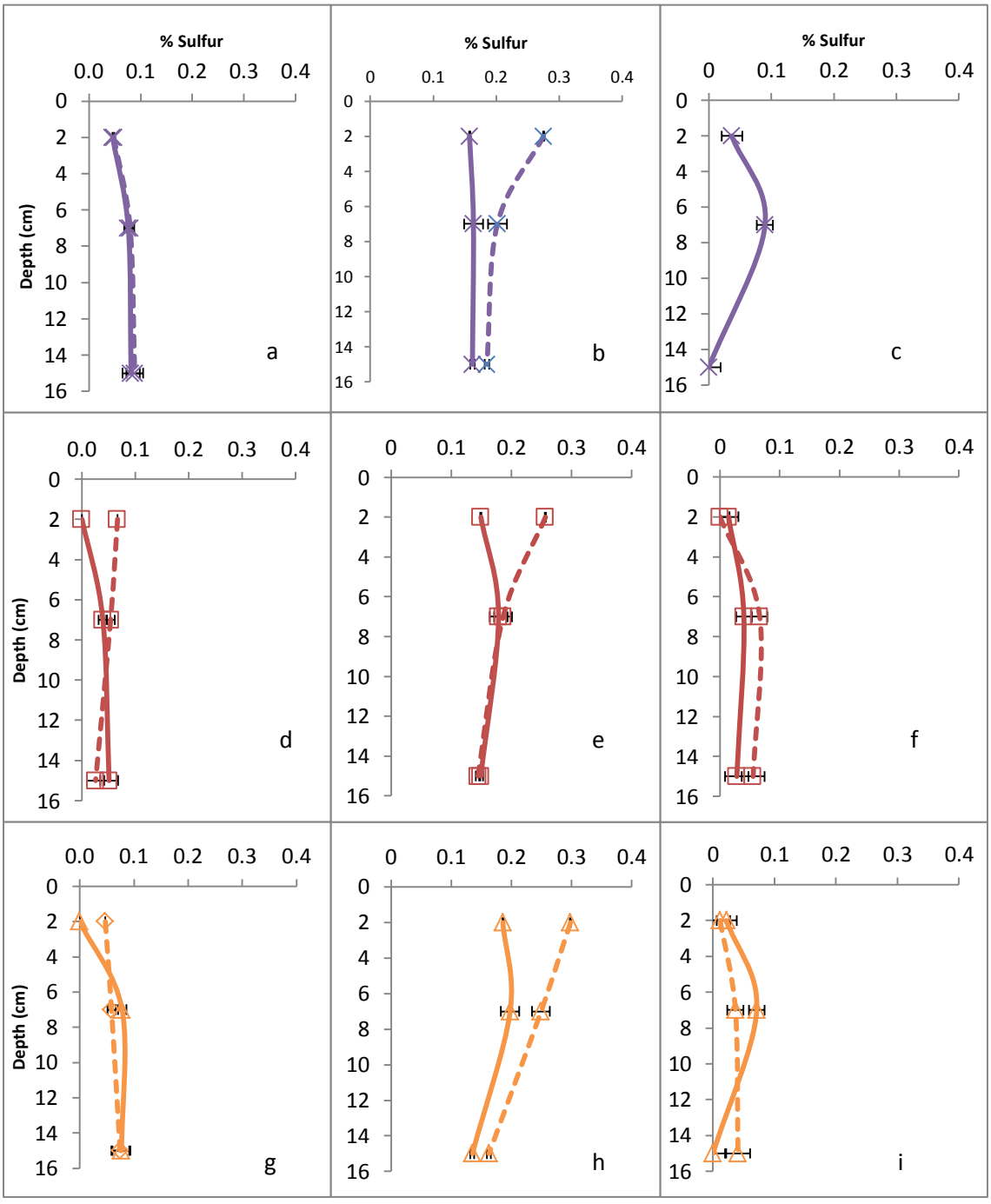

Figure 9. Sediment profiles of Initial (dotted lines) and final (solid lines) for LEF (a, d, and g), SB (b, e, and h), and UEF (c, f, and i) % sulfur concentrations. High sulfate treatments (a-c) are displayed in purple crosses, medium treatments (d-f) are displayed in red squares and low treatments (g-i) are displayed in yellow triangles.

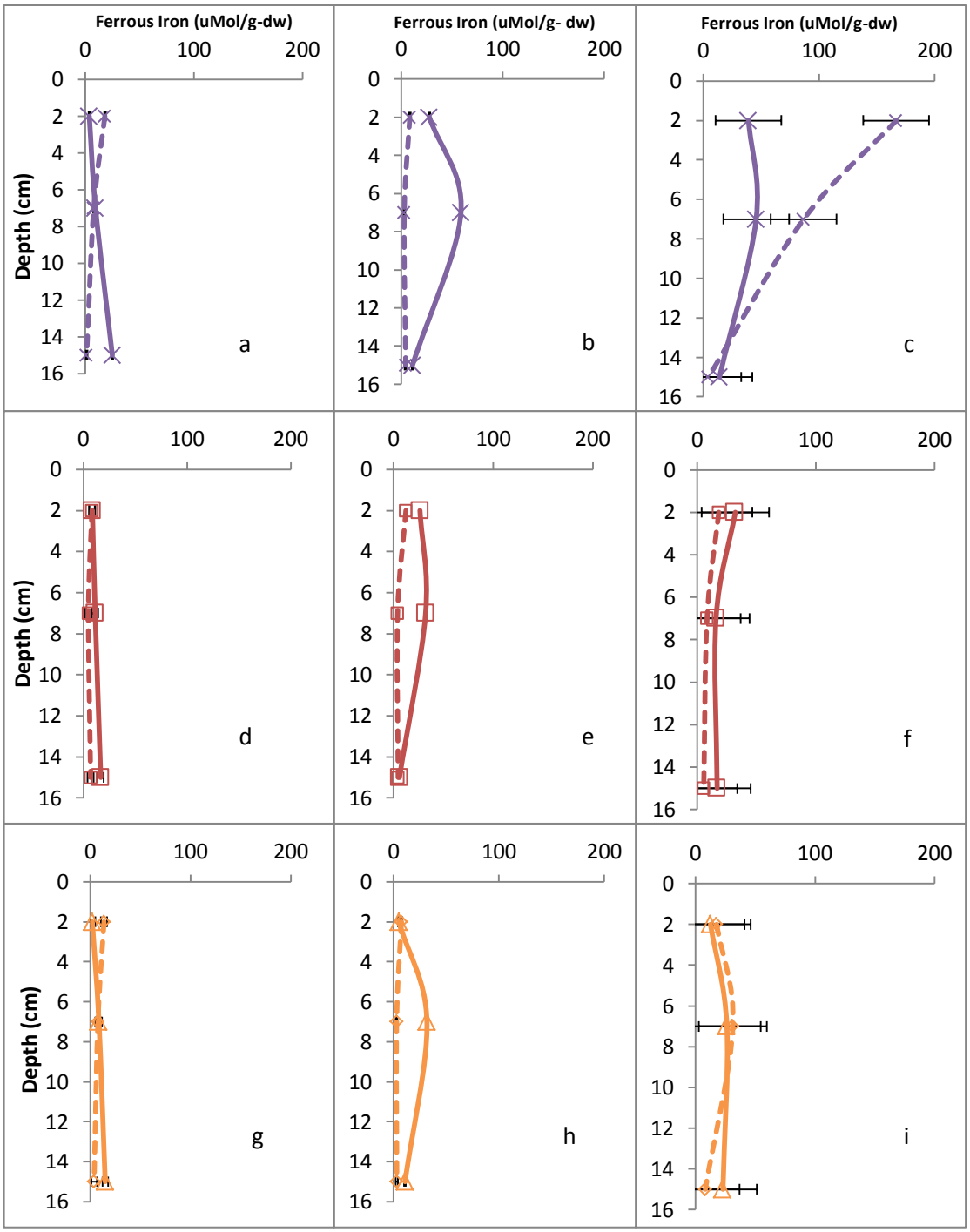

Figure 10. Sediment ferrous iron concentration profiles of Initial (dotted lines) and final (solid lines) for LEF (a, d, and g), SB (b, e, and h), and UEF (c, f, and i) experimental conditions. High sulfate treatments (a-c) are displayed in purple crosses, medium treatments (d-f) are displayed in red squares and low treatments (g-i) are displayed in yellow triangles.

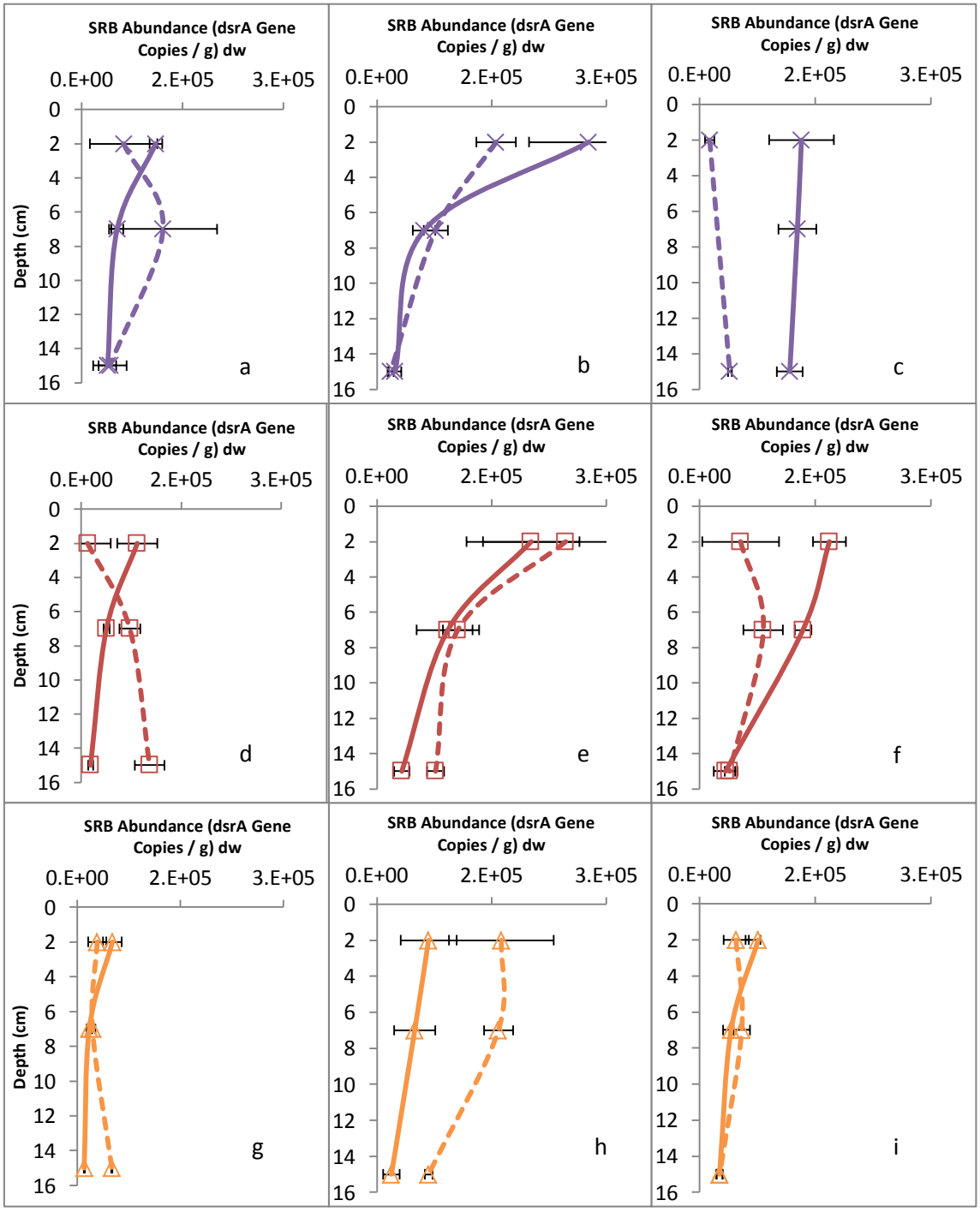

Figure 11. Sediment SRB abundance profiles of Initial (dotted lines) and final (solid lines) for LEF (a, d, and g), SB (b, e, and h), and UEF (c, f, and i). High sulfate treatments (a-c) are displayed in purple crosses, medium treatments (d-f) are displayed in red squares and low (g-i) are displayed in yellow triangles.

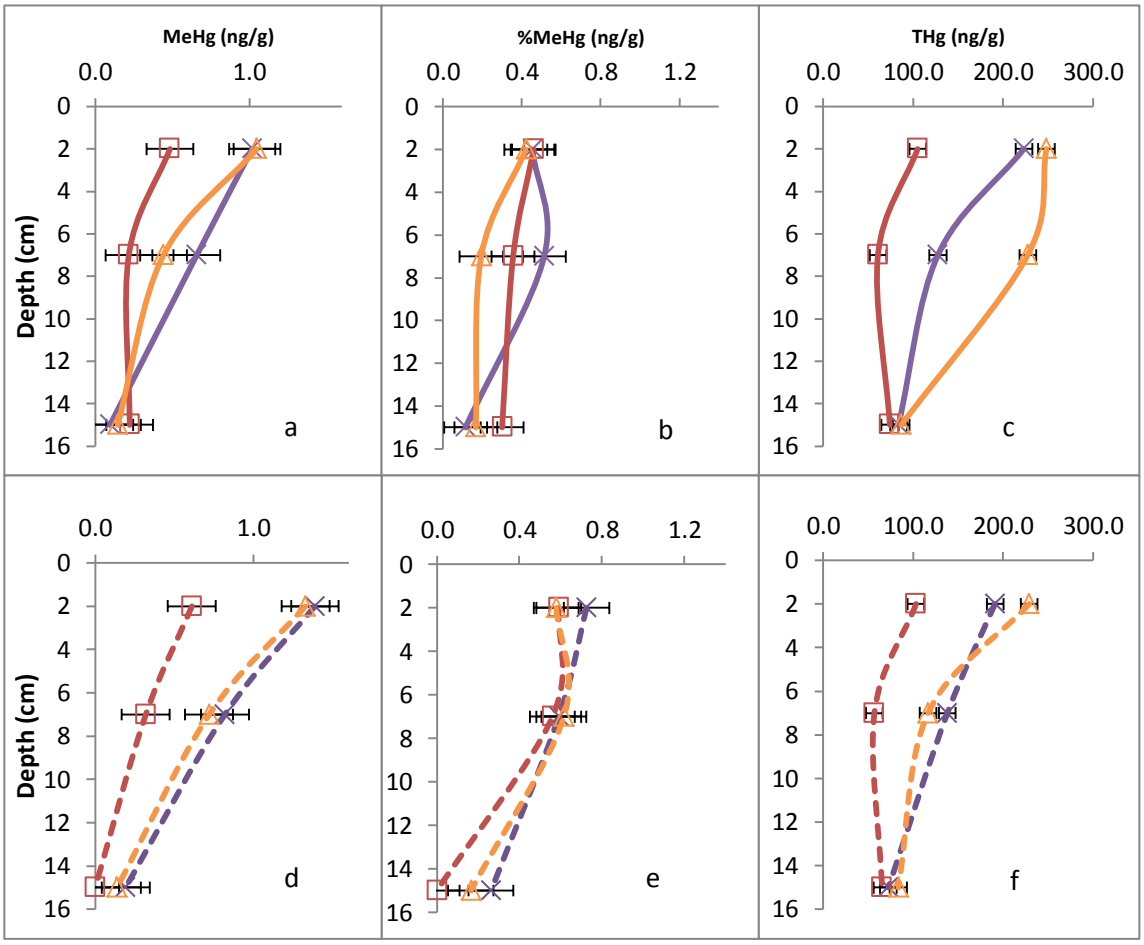

Figure 12. LEF sediment solid phase MeHg (a and d), %MeHg (b and e), and THg (c and f) for the LEF high (purple cross), medium (red square), and low (orange triangle) sulfate treatments at experimental initial conditions (dotted lines; d-f) and final conditions (solid lines; a-c). Error bars represent one standard deviation from the mean as calculated by the analysis of triplicate sub-cores from each habitat zone at the beginning of experiments.

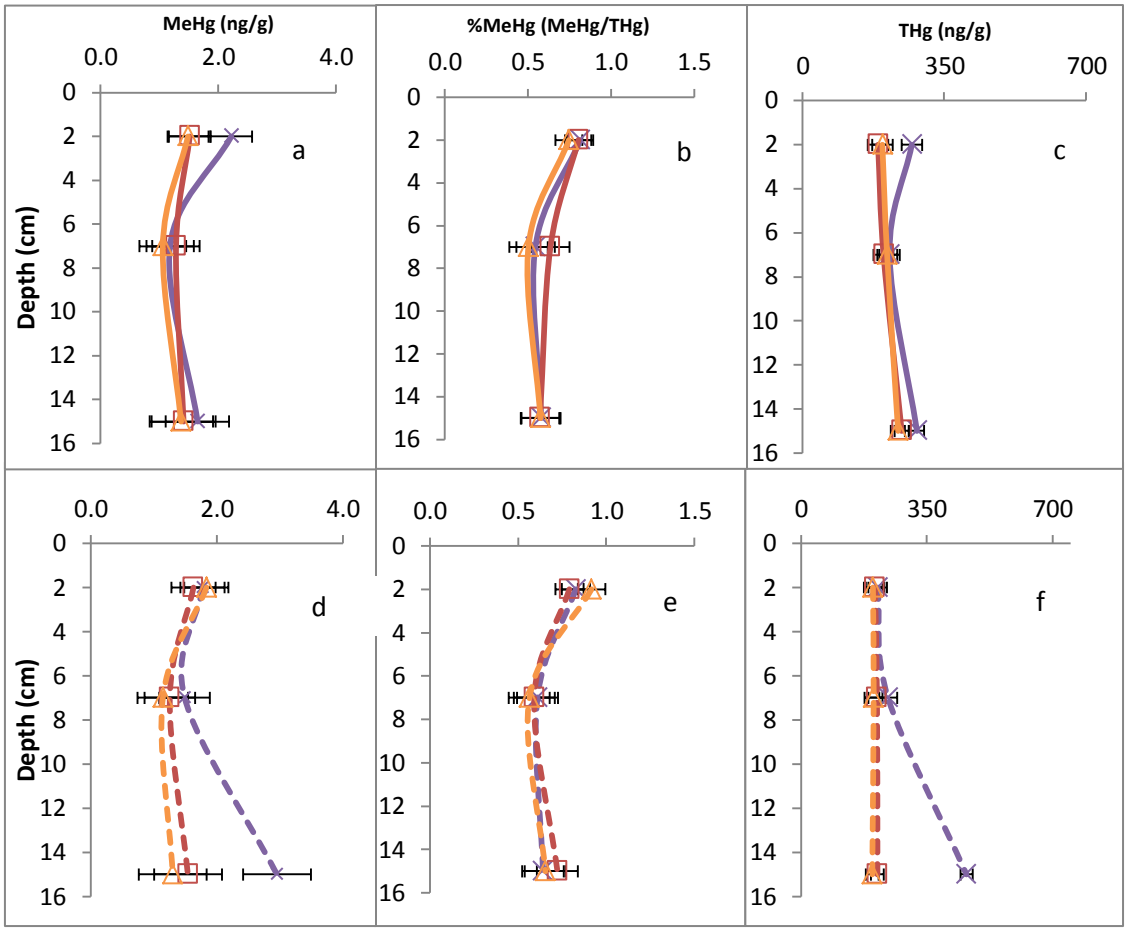

Figure 13. SB sediment solid phase MeHg (a and d), %MeHg (b and e), and THg (c and f) for the LEF high (purple cross), medium (red square), and low (orange triangle) sulfate treatments at experimental initial conditions (dotted lines; d-f) and final conditions (solid lines; a-c). Error bars represent one standard deviation from the mean as calculated by the analysis of triplicate sub-cores from each habitat zone at the beginning of experiments.

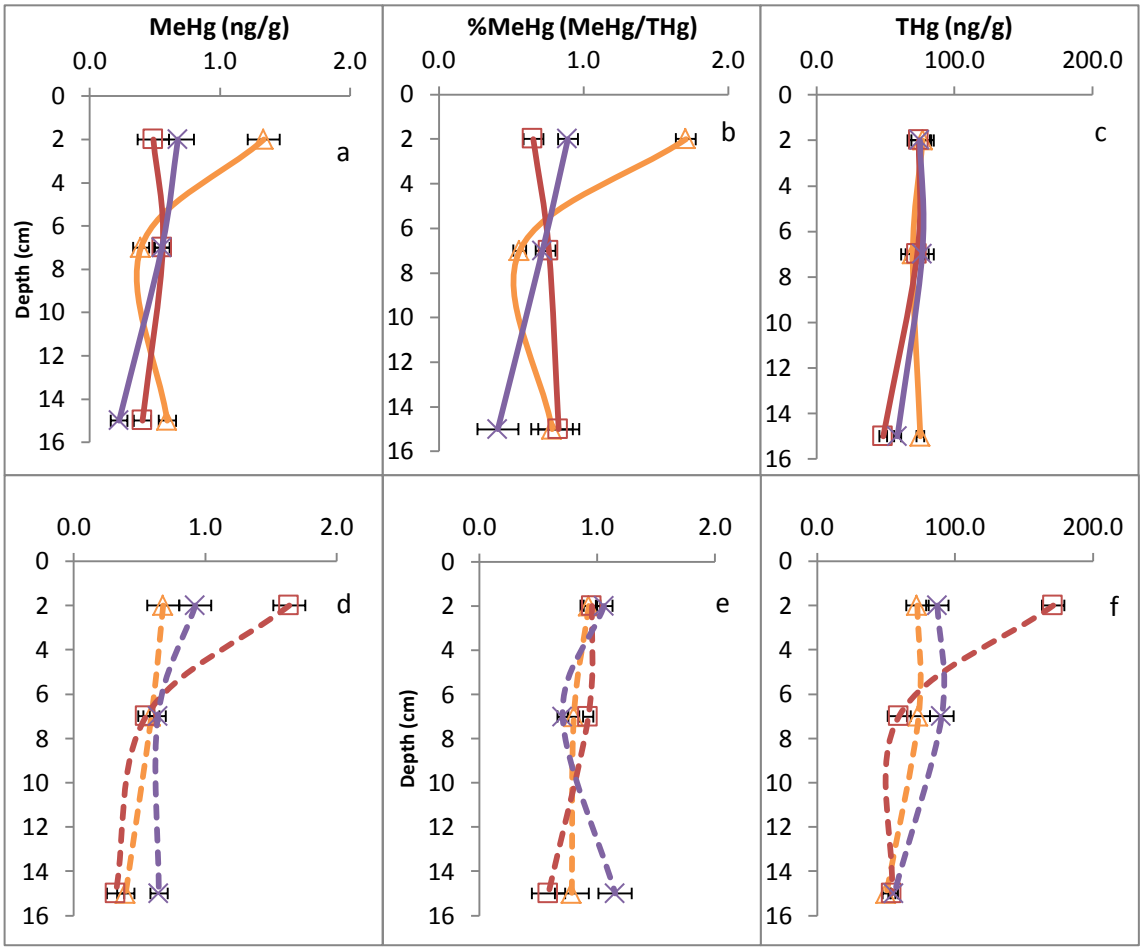

Figure 14. UEF sediment solid phase MeHg (a and d), %MeHg (b and e), and THg (c and f) for the LEF high (purple cross), medium (red square), and low (orange triangle) sulfate treatments at experimental initial conditions (dotted lines; d-f) and final conditions (solid lines; a-c). Error bars represent one standard deviation from the mean as calculated by the analysis of triplicate sub-cores from each habitat zone at the beginning of experiments.

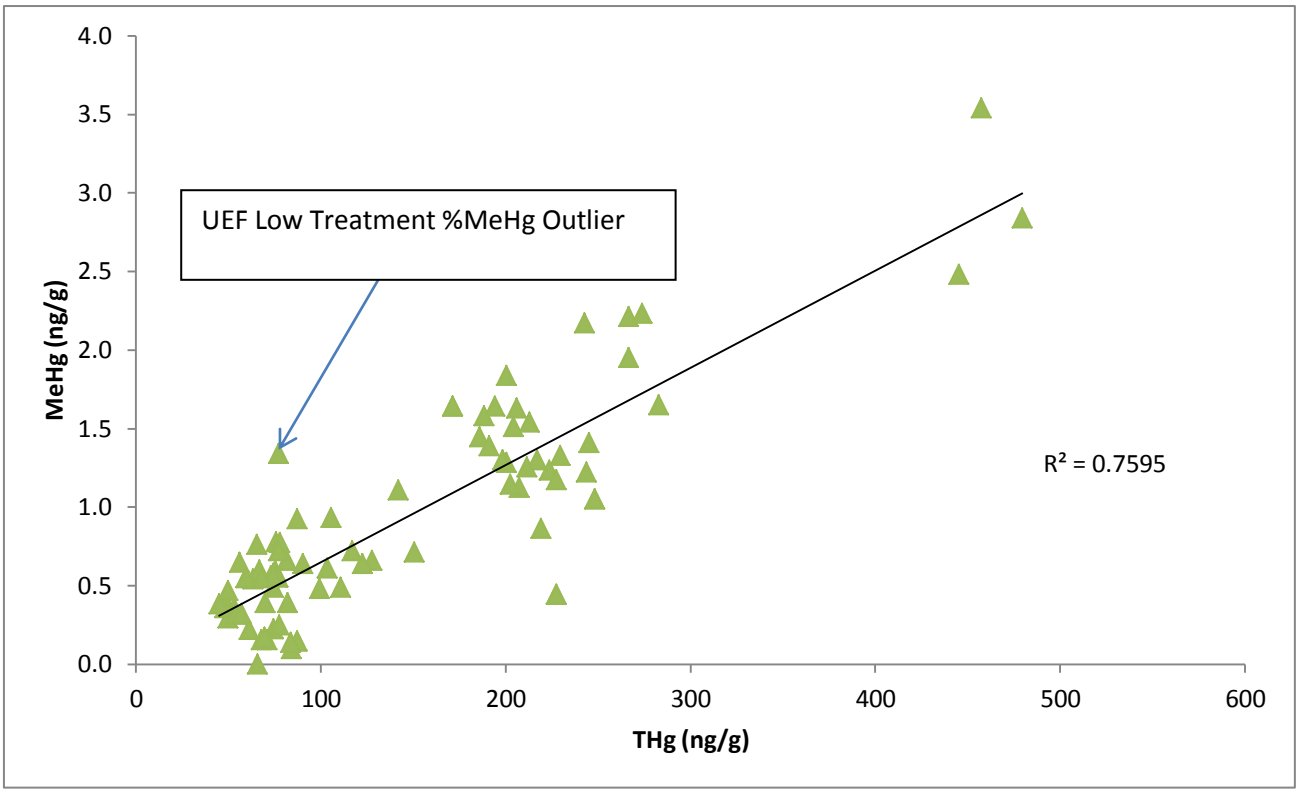

Figure 15. Relationship between THg and MeHg for all habitat zones sampled. R^2 value is labeled next to regression line. THg and MeHg were significantly correlated ($p < 0.05$) in the St. Louis River Estuary.

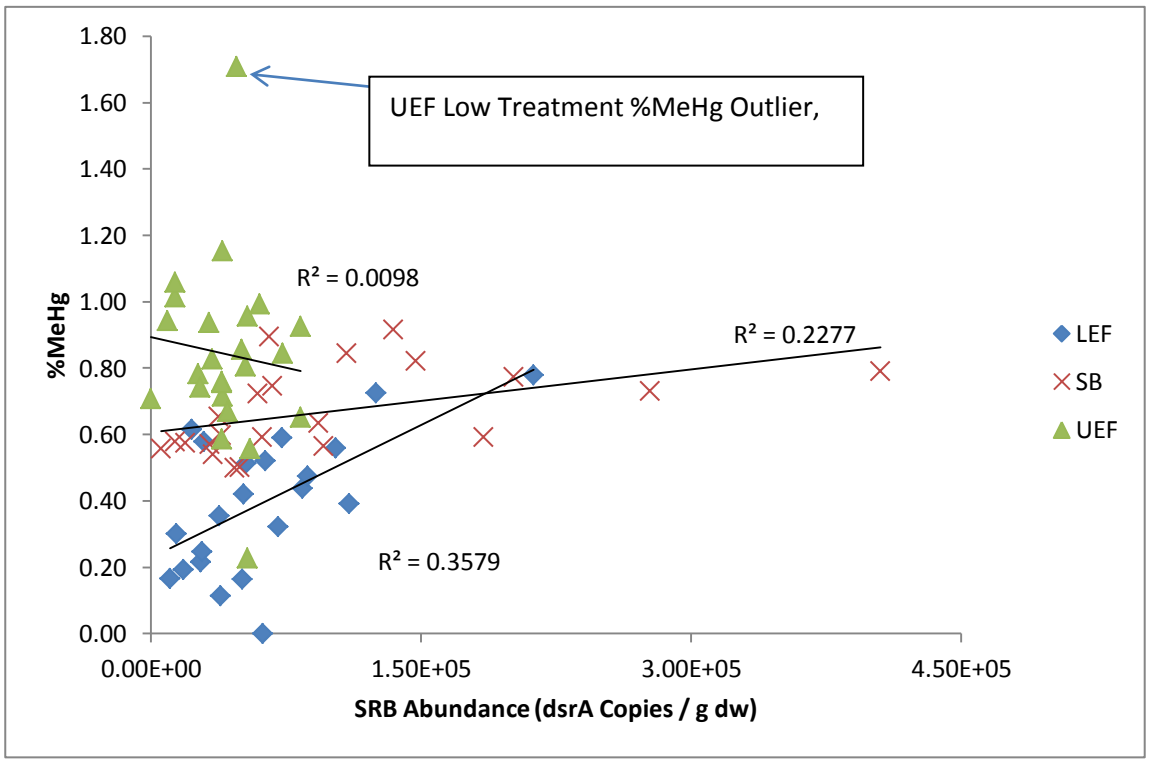

Figure 16. Relationship between % MeHg and SRB Abundance for LEF (blue), UEF (green), and SB (red) habitat zones. R^2 values are labeled next to the regression line they represent.

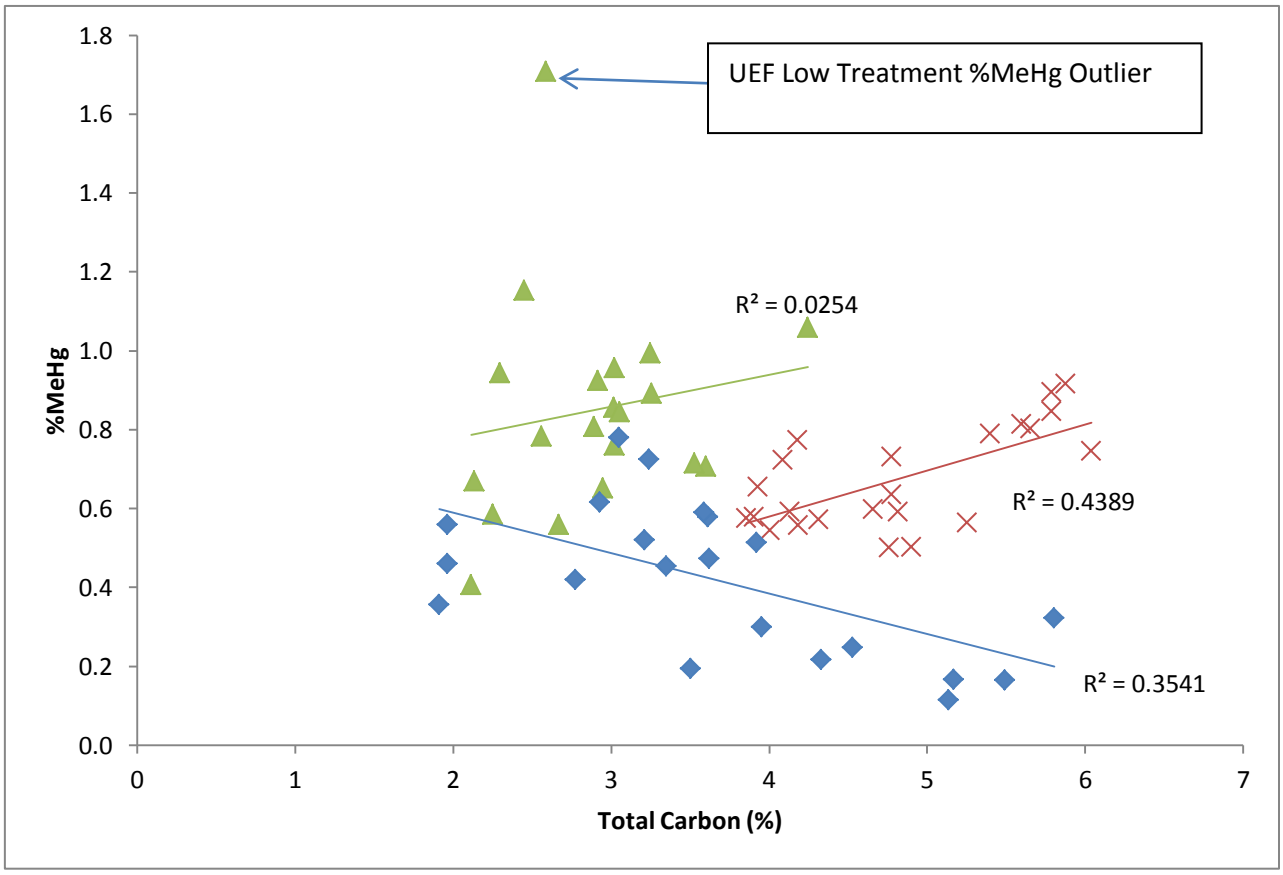

Figure 17. Relationship between % MeHg and TC Abundance for LEF (blue), UEF (green), and SB (red) habitat zones. R^2 and p values are labeled next to the regression line they represent.

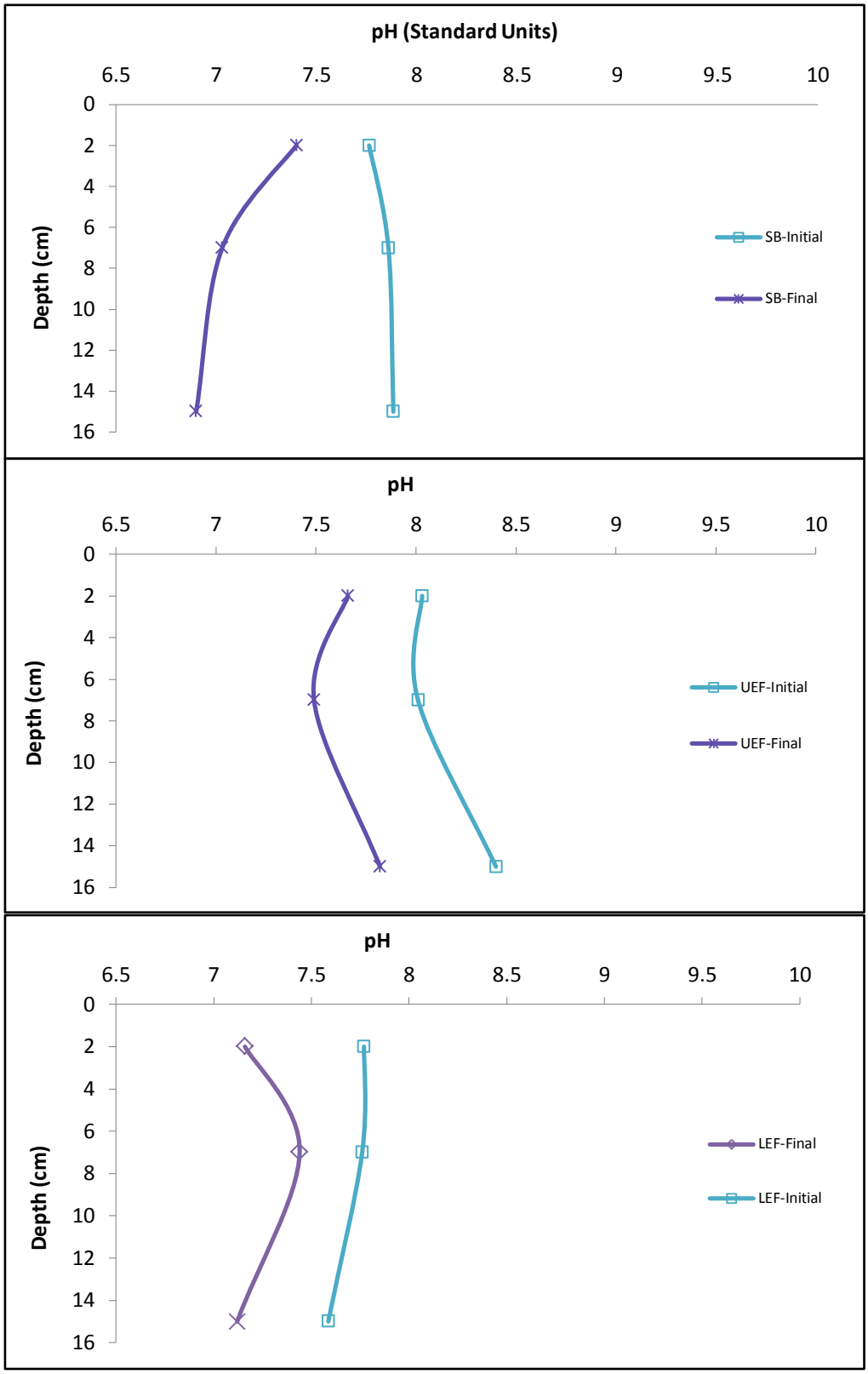

Figure 18 pH in sediment microcosms. pH was measured within 6hr of collecting sediment for final sampling, but 24hours later for initial sampling.

Table 1. K_D values tabulated for THg in the top 10 cm of each habitat zone. Flux values were also determined for each habitat zone for THg.

Habitat Zone	Porewater THg (ng L^{-1})	Solid Phase THg (ng g^{-1})	THg log(K_D)	Thg Flux (ng m^{-2} d^{-1})
UEF	12.27±5.37	89.18±23.37	3.88±0.13	18.50±5.98
SB	4.48±1.80	209.77±7.87	4.70±0.20	15.47±7.94
LEF	26.29±21.63	176.8±83.75	3.88±0.20	38.16±9.08

Table 2 K_D values tabulated for MeHg in the top 10 cm of each habitat zone. Flux values for MeHg were below detection limits and not reported.

Habitat Zone	Porewater MeHg (ng L^{-1})	Solid Phase MeHg (ng g^{-1})	MeHg Log(K_D)
UEF	0.33±0.07	0.52±0.02	3.20±0.51
SB	0.32±0.04	1.42±0.18	3.65±0.18
LEF	0.46±0.55	0.76±0.36	3.42±0.45

Table 3 MeHg values calculated for mass transfer coeficients (K_{mt}), Flux, and MeHg Load for each habitat zone.

Habitat Zone	Calculated K_{mt}	Overlying Water (ng L^{-1})	Estimated Flux (ng m^{-2} d^{-1})	Area (km^2)	MeHg Load (mg hr^{-1})	Inorganic Hg Load (mg hr^{-1})
UEF	1.86	0.09±0.07	0.45	8.27	3.70	149.2
SB	6.12	0.05±0.04	1.68	3.59	6.05	49.49
LEF	2.34	0.12±0.14	0.79	10.53	8.31	393.6

Table 4 MeHg and THg concentration measured at the Scanlon Dam in Cloquet Dam taken from Berndt and Bavin (2009), and Berndt and Bavin (2012). MeHg load calculated from USGS flow data obtained on the same day MeHg water sample was taken.

Site	Concentration MeHg (ng L^{-1})	Concentration THg (ng L^{-1})	Flow Rate (L s^{-1})	MeHg Load (mg hr^{-1})	Inorganic Hg Load (mg hr^{-1})
Scanlon Dam	0.15	2.0	28317	15.29	188.6
Scanlon Dam	0.3	6.4	311485	336.4	6840
Scanlon Dam	0.187	3.22	193687	130.4	2115
Scanlon Dam	0.09	2.5	22285	7.22	193.3